Leaf-scale quantification of the effect of photosynthetic gas exchange on $\delta^{17}O$ of atmospheric CO_2

Adnew, Getachew Agmuas; Pons, Thijs L.; Koren, Gerbrand; Peters, Wouter; Rockmann, Thomas

Published in:
Biogeosciences

DOI:
10.5194/bg-17-3903-2020

Publication date:
2020

Biogeosciences, 17, 3903–3922, 2020
https://doi.org/10.5194/bg-17-3903-2020

Biogeosciences Open Access EGU

Leaf-scale quantification of the effect of photosynthetic gas exchange on $\Delta^{17}O$ of atmospheric CO_2

Getachew Agmuas Adnew[1], **Thijs L. Pons**[2], **Gerbrand Koren**[3], **Wouter Peters**[3,4], **and Thomas Röckmann**[1]

[1]Institute for Marine and Atmospheric research Utrecht (IMAU), Utrecht University, Utrecht, the Netherlands
[2]Institute of Environmental Biology, Utrecht University, Utrecht, the Netherlands
[3]Department of Meteorology and Air Quality, Wageningen University, Wageningen, the Netherlands
[4]Centre for Isotope Research, University of Groningen, Groningen, the Netherlands

Correspondence: Getachew Agmuas Adnew (g.a.adnew@uu.nl)

Received: 23 March 2020 – Discussion started: 27 March 2020
Revised: 22 May 2020 – Accepted: 18 June 2020 – Published: 31 July 2020

Abstract. Understanding the processes that affect the triple oxygen isotope composition of atmospheric CO_2 during gas exchange can help constrain the interaction and fluxes between the atmosphere and the biosphere. We conducted leaf cuvette experiments under controlled conditions using three plant species. The experiments were conducted at two different light intensities and using CO_2 with different $\Delta^{17}O$. We directly quantify the effect of photosynthesis on $\Delta^{17}O$ of atmospheric CO_2 for the first time. Our results demonstrate the established theory for $\delta^{18}O$ is applicable to $\Delta^{17}O(CO_2)$ at leaf level, and we confirm that the following two key factors determine the effect of photosynthetic gas exchange on the $\Delta^{17}O$ of atmospheric CO_2. The relative difference between $\Delta^{17}O$ of the CO_2 entering the leaf and the CO_2 in equilibrium with leaf water and the back-diffusion flux of CO_2 from the leaf to the atmosphere, which can be quantified by the c_m/c_a ratio, where c_a is the CO_2 mole fraction in the surrounding air and c_m is the one at the site of oxygen isotope exchange between CO_2 and H_2O. At low c_m/c_a ratios the discrimination is governed mainly by diffusion into the leaf, and at high c_m/c_a ratios it is governed by back-diffusion of CO_2 that has equilibrated with the leaf water. Plants with a higher c_m/c_a ratio modify the $\Delta^{17}O$ of atmospheric CO_2 more strongly than plants with a lower c_m/c_a ratio. Based on the leaf cuvette experiments, the global value for discrimination against $\Delta^{17}O$ of atmospheric CO_2 during photosynthetic gas exchange is estimated to be -0.57 ± 0.14 ‰ using c_m/c_a values of 0.3 and 0.7 for C_4 and C_3 plants, respectively. The main uncertainties in this global estimate arise from variation in c_m/c_a ratios among plants and growth conditions.

1 Introduction

Stable isotope measurements of CO_2 provide important information about the magnitude of the CO_2 fluxes between atmosphere and biosphere, which are the largest components of the global carbon cycle (Farquhar et al., 1989, 1993; Ciais et al., 1997a, b; Flanagan and Ehleringer, 1998; Yakir and Sternberg, 2000; Gillon and Yakir, 2001; Cuntz et al., 2003a, b). A better understanding of the terrestrial carbon cycle is essential for predicting future climate and atmospheric CO_2 mole fractions (Booth et al., 2012). Gross primary productivity (GPP), the total carbon dioxide uptake by vegetation during photosynthesis, can only be determined indirectly and remains poorly constrained (Cuntz, 2011; Welp et al., 2011). For example, Beer et al. (2010) estimated global GPP to be 102–135 $PgC\,yr^{-1}$ (85 % confidence interval, CI) using machine learning techniques by extrapolating from a database of eddy covariance measurements of CO_2. This estimate has since then been widely used as target for terrestrial vegetation models (Sitch et al., 2015) and replicated based on cross-consistency checks with atmospheric inversions, sun-induced fluorescence (SIF), and global vegetation models (Jung et al., 2020). As an alternative, Welp et al. (2011) estimated global GPP to be 150–175 $PgC\,yr^{-1}$ using variations in $\delta^{18}O$ of atmospheric CO_2 after the 1997/98 El Niño event; see Eq. (1) for definition of the δ value.

The concept behind the latter study was that atmospheric CO_2 exchanges oxygen isotopes with leaf and soil water, and this isotope exchange mostly determines the observed variations in $\delta^{18}O$ of CO_2 (Francey and Tans, 1987; Yakir, 1998).

Following the 97/98 El Niño–Southern Oscillation (ENSO) event, the anomalous $\delta^{18}O$ signature imposed on tropical leaf and soil waters was transferred to atmospheric CO_2, before slowly disappearing as a function of the lifetime of atmospheric CO_2. This in turn is governed by the land vegetation uptake of CO_2 during photosynthesis, as well as soil invasion of CO_2 (Miller et al., 1999; Wingate et al., 2009). For the photosynthesis term, the equilibration of CO_2 with water is an uncertain parameter in this calculation, partly because the $\delta^{18}O$ of water at the site of isotope exchange in the leaf is not well defined. Importantly, a significant $\delta^{18}O$ variation can occur in leaves due to the preferential evaporation of $H_2^{16}O$ relative to $H_2^{18}O$ (Gan et al., 2002, 2003; Farquhar and Gan, 2003; Cernusak et al., 2016), which induces a considerable uncertainty in estimating $\delta^{18}O$ of CO_2. Similar considerations for the transfer of the $\delta^{18}O$ signature of precipitation into the soils, and then up through the roots, stems, and leaves makes ^{18}O of CO_2 a challenging measurement to interpret (Peylin et al., 1999; Cuntz et al., 2003a, b).

Classical isotope theory posits that oxygen isotope distributions are modified in a mass-dependent way. This means that the $^{17}O/^{16}O$ ratio changes by approximately half of the corresponding change in $^{18}O/^{16}O$ (Eq. 2), and it applies to the processes involved in gas exchange between atmosphere and plants. However, in 1983 Thiemens and coworkers (Heidenreich and Thiemens, 1983, 1986; Thiemens and Heidenreich, 1983) reported a deviation from mass-dependent isotope fractionation in ozone (O_3) formation called mass-independent isotope fractionation ($\Delta^{17}O$, Eq. 3). In the stratosphere, the $\Delta^{17}O$ of O_3 is transferred to CO_2 via isotope exchange of CO_2 with $O(^1D)$ produced from O_3 photolysis (Yung et al., 1991, 1997; Shaheen et al., 2007), which results in a large amount of $\Delta^{17}O$ in stratospheric CO_2 (Thiemens et al., 1991, 1995; Lyons, 2001; Lämmerzahl et al., 2002; Thiemens, 2006; Kawagucci et al., 2008; Wiegel et al., 2013).

Once $\Delta^{17}O$ has been created in stratospheric CO_2, the only process that modify its signal is isotope exchange with leaf water, soil water and ocean water at the Earth's surface, after CO_2 has reentered the troposphere (Boering, 2004; Thiemens et al., 2014; Liang and Mahata, 2015; Hofmann et al., 2017). Isotope exchange with leaf water is more efficient relative to ocean water due to the presence of the enzyme carbonic anhydrase (CA), which effectively catalyzes the conversion of CO_2 and H_2O to HCO_3^- and H^+ and vice versa (Francey and Tans, 1987; Friedli et al., 1987; Badger and Price, 1994; Gillon and Yakir, 2001). The isotope exchange in the atmosphere is negligible due to lower liquid water content, lower residence time, and the absence of carbonic anhydrase (Mills and Urey, 1940; Miller et al., 1971; Johnson, 1982; Silverman, 1982; Francey and Tans, 1987).

$\Delta^{17}O$ of CO_2 has been suggested as an additional independent tracer for constraining global GPP (Hoag et al., 2005; Thiemens et al., 2013; Hofmann et al., 2017; Liang et al., 2017b; Koren et al., 2019) because the processes involved in plant–atmosphere gas exchange are all mass dependent. Therefore, $\Delta^{17}O$ at the CO_2-H_2O exchange site in the leaf will vary much less than $\delta^{18}O$. Nevertheless, mass-dependent isotope fractionation processes with slightly different three-isotope fractionation slopes are involved, which have been precisely established in the past years. Figure 1 shows how the different processes affect $\Delta^{17}O$ of the H_2O and CO_2 reservoirs involved. The triple isotope slope of oxygen in meteoric waters is taken as reference slope, $\lambda_{Ref} = 0.528$ (Meijer and Li, 1998; Barkan and Luz, 2007; Landais et al., 2008; Luz and Barkan, 2010; Uemura et al., 2010), and we assume that soil water is similar to meteoric water. Due to transpiration and diffusion in the leaf, $\Delta^{17}O$ of leaf water gets modified following a humidity-dependent three-isotope slope $\theta_{trans} = 0.522 - 0.008 \times h$ (Landais et al., 2006). Exchange of oxygen isotopes between leaf water and CO_2 follows $\theta_{CO_2-H_2O} = 0.5229$ (Barkan and Luz, 2012), which determines the $\Delta^{17}O$ of CO_2 inside the leaf at the CO_2-H_2O exchange site. Finally, the $\Delta^{17}O$ of the CO_2 is modified when CO_2 diffuses into and out of the leaf with $\lambda_{diff} = 0.509$ (Young et al., 2002).

In the first box model study of Hoag et al. (2005), the small deviations in $\Delta^{17}O$ of CO_2 due to differences in three-isotope slopes were neglected and exchange with water was assumed to reset $\Delta^{17}O$ to 0. Hofmann et al. (2017) included the different isotope effects shown in Fig. 1 in their box model. Koren et al. (2019) incorporated all the physicochemical processes affecting $\Delta^{17}O$ of CO_2 in a 3D atmospheric model and investigated the spatiotemporal variability of $\Delta^{17}O$ and its use as tracer for GPP. Using these and other similar models, numerous measurements of $\Delta^{17}O$ in atmospheric CO_2 from different locations have been performed and used to estimate GPP (Liang et al., 2006; Barkan and Luz, 2012; Thiemens et al., 2014; Liang and Mahata, 2015; Laskar et al., 2016; Hofmann et al., 2017). The three-isotope slopes of the processes involved in the gas exchange (Fig. 1) have been precisely determined in idealized experiments. In the advanced models mentioned above it is assumed that when all the pieces are put together they result in a realistic overall modification of $\Delta^{17}O$ of CO_2 in the atmosphere surrounding the leaf. However, this has not been confirmed by measurements previously.

In this study we report the effect of photosynthesis on $\Delta^{17}O$ of CO_2 in the surrounding air at the leaf scale. We measured $\Delta^{17}O$ of CO_2 entering and leaving a leaf cuvette to calculate the isotopic fractionation associated with photosynthesis for three species that are representative for three different biomes. The fast-growing annual herbaceous C_3 species *Helianthus annuus* (sunflower) has a high photosynthetic capacity (A_n) and high stomatal conductance (g_s) and is representative for temperate and tropical crops (Fredeen et al., 1991). The slower-growing perennial evergreen C_3 species *Hedera hibernica* (ivy) is representative of forests and other woody vegetation and stress-subjected habitats (Pons et al., 2009). The fast-growing, agronomically im-

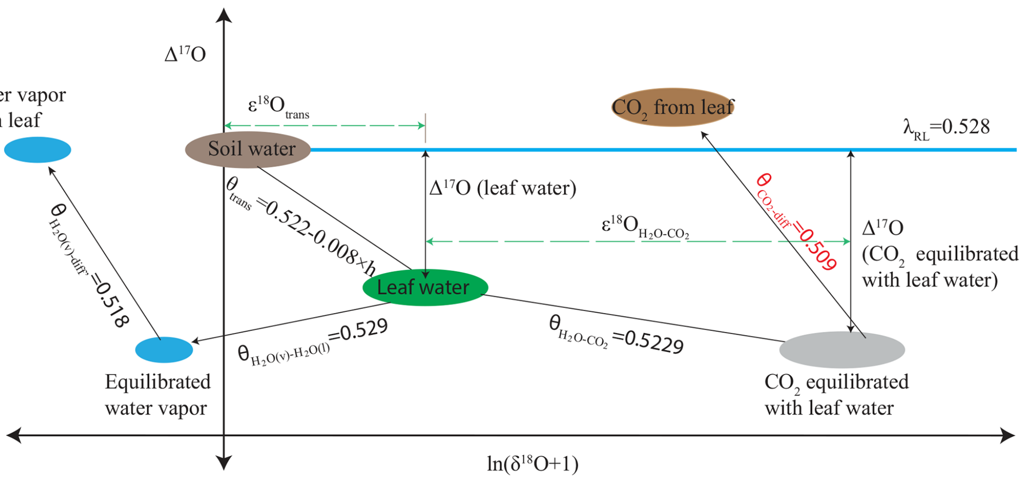

Figure 1. Schematic for mass-dependent isotope fractionation process that affects the $\Delta^{17}O$ of the CO_2 and H_2O during the photosynthetic gas exchange (not to scale). The triple oxygen isotope relationships for the individual isotope fractionation processes (both kinetic and equilibrium fractionation) are assigned with θ. $\theta_{trans} = 0.522 - 0.008 \times h$, where h is relative humidity (Landais et al., 2006). In this study the humidity is 75 %, $\theta_{trans} = 0.516$, $\theta_{CO_2-H_2O}$ (Barkan and Luz, 2012), θ_{CO_2-diff} (Young et al., 2002), $\theta_{H_2O(v)-H_2O(l)}$ (Barkan and Luz, 2005), and $\theta_{H_2O(v)-diff}$ (Barkan and Luz, 2007), where v and l are vapor and liquid water, respectively. $\varepsilon^{18}O$ is enrichment or depletion in ^{18}O isotope composition due to the corresponding isotope fractionation process, and diff and trans stand for diffusion and transpiration, respectively.

portant crop *Zea mays* (maize) is an herbaceous annual C_4 species with a high A_n and a low g_s, typical for savanna type vegetation (van der Weijde et al., 2013). The mole fraction of CO_2 at the CO_2-H_2O exchange site (c_m) is an important parameter to determine the effect of photosynthesis on $\Delta^{17}O$ of CO_2. In C_3 plants, the CO_2-H_2O exchange can occur anywhere between the plasma membrane and the chloroplast since the catalyzing enzyme CA has been found in the chloroplast, cytosol, mitochondria, and plasma membrane (Fabre et al., 2007; DiMario et al., 2016). For C_4 plants, CA is mainly found in the cytosol, and the CO_2-H_2O exchange occurs there (Badger and Price, 1994). In our experiments, sunflower and ivy are used to cover the wide c_m/c_a ratio range among C_3 plants and maize represents the c_m/c_a ratio for the C_4 plants. Using our results from the leaf-scale experiments, we estimated the effect of terrestrial vegetation on $\Delta^{17}O$ of CO_2 in the global atmosphere.

2 Theory

2.1 Notation and definition of δ values

Isotopic composition is expressed as the deviation of the heavy-to-light isotope ratio in a sample relative to a reference ratio and is denoted as δ, expressed in per mill (‰). In the case of oxygen isotopes, the isotope ratios are $^{18}R=[^{18}O]/[^{16}O]$ and $^{17}R=[^{17}O]/[^{16}O]$ and the reference material is Vienna Standard Mean Ocean Water (VSMOW):

$$\delta^{n}O = \frac{^{n}R_{sample}}{^{n}R_{VSMOW}} - 1, \quad n \text{ refers to } 17 \text{ or } 18. \tag{1}$$

For most processes, isotope fractionation depends on mass, and therefore the fractionation against ^{17}O is approximately half of the fractionation against ^{18}O (Eq. 3).

$$\ln\left(\delta^{17}O + 1\right) = \lambda \times \ln\left(\delta^{18}O + 1\right) \tag{2}$$

The mass-dependent isotope fractionation factor λ ranges from 0.5 to 0.5305 for different molecules and processes (Matsuhisa et al., 1978; Thiemens, 1999; Young et al., 2002; Cao and Liu, 2011). $\Delta^{17}O$ is used to quantify the degree of deviation from Eq. (2) (see Eq. 3). Note that $\Delta^{17}O$ changes not only by mass-independent isotope fractionation processes but also by mass-dependent isotope fractionation processes with a different λ value from the one used in the definition of $\Delta^{17}O$ (Barkan and Luz, 2005, 2011; Landais et al., 2006, 2008; Luz and Barkan, 2010; Pack and Herwartz, 2014).

$$\Delta^{17}O = \ln\left(\delta^{17}O + 1\right) - \lambda \times \ln\left(\delta^{18}O + 1\right) \tag{3}$$

The choice of λ is in principle arbitrary, and in this study we use $\lambda = 0.528$, which was established for meteoric waters (Meijer and Li, 1998; Landais et al., 2008; Brand et al., 2010; Luz and Barkan, 2010; Barkan and Luz, 2012; Sharp et al., 2018). Equation (3) can be linearized to $\Delta^{17}O = \delta^{17}O - \lambda \times \delta^{18}O$ (Miller, 2002), but this approximation causes an error that increases with $\delta^{18}O$ (Miller, 2002; Bao et al., 2016).

2.2 Discrimination against $\Delta^{17}O$ of CO_2

The overall isotope fractionation associated with the photosynthesis of CO_2 is commonly quantified using the term discrimination, as described in Farquhar and Richards (1984), Farquhar et al. (1989), and Farquhar and Lloyd (1993). We use the symbol Δ_A for discrimination due to assimilation in this paper since the commonly used Δ is already used for the definition of $\Delta^{17}O$ (see Eq. 3). Δ_A quantifies the enrichment or depletion of carbon and oxygen isotopes of CO_2 in the surrounding atmosphere relative to the CO_2 that is assimilated (Farquhar and Richards, 1984). It can be calculated from the isotopic composition of the CO_2 entering and leaving the leaf cuvette (Evans et al., 1986; Gillon and Yakir, 2000a; Barbour et al., 2016) as follows:

$$\Delta_A^n O_{obs} = \frac{^nR_a}{^nR_A} - 1 = \frac{^nO_a - \delta^n O_A}{1 + \delta^n O_A} = \frac{\zeta \times (\delta^n O_a - \delta^n O_e)}{1 + \delta^n O_a - \zeta \times (\delta^n O_a - \delta^n O_e)}, \tag{4}$$

where the indices e, a and A refer to CO_2 entering and leaving the cuvette and being assimilated, respectively. $\zeta = \frac{c_e}{c_e - c_a}$, where c_e and c_a are the mole fractions of CO_2 entering and leaving the cuvette. For quantifying the effect of photosynthesis on $\Delta^{17}O$ in our experiments, the $\Delta_A\Delta^{17}O$ is calculated from $\Delta_A^{17}O$ and $\Delta_A^{18}O$ using the three-isotope slope $\lambda_{RL} = 0.528$, similar to Eq. (3). In previous studies slightly different formulations have been used to define the effect of photosynthesis on $\Delta^{17}O$, and a comparison of the different definitions is provided in the Supplement (Eqs. S37–S40).

It is important to note that when the logarithmic definition of $\Delta^{17}O$ or $\Delta_A\Delta^{17}O$ is used, values are not additive (Kaiser et al., 2004). In linear calculations, the error gets larger when the relative difference in $\delta^{18}O$ between the two CO_2 gases increases regardless of the $\Delta^{17}O$ of the individual CO_2 gases (Fig. S1 in the Supplement). Therefore, $\Delta_A\Delta^{17}O$ values have to be calculated from the individual $\Delta_A^{17}O$ and $\Delta_A^{18}O$ values and not by linear combinations of the $\Delta^{17}O$ of air entering and leaving a plant chamber.

3 Materials and methods

3.1 Plant material and growth conditions

Sunflower (*Helianthus annuus* L. cv "sunny") was grown from seeds in 0.6 L pots with potting soil (Primasta, the Netherlands) for about 4 weeks. All leaves appearing above the first leaf pair were removed to avoid shading. Established juvenile ivy (*Hedera hibernica* L.) plants were pruned and planted in 6 L pots for 6 weeks. Ivy leaves that had developed and matured were used for the experiments. Maize (*Z. mays* L. cv "saccharate") was grown from seed in 1.6 L pots for at least 7 weeks. For maize, the fourth or higher leaf number was used for the experiments when it was mature. A section of the leaf at about one-third from the tip was inserted into the leaf cuvette. They were placed on a subirrigation system that provided water during the growth period in a controlled-environment growth chamber, with an air temperature of 20 °C, relative humidity of 70 %, and CO_2 mole fraction of about 400 ppm. The photosynthetic photon flux density (PPFD) was about 300 $\mu mol\,m^{-2}\,s^{-1}$ during a daily photoperiod of 16 h measured with a PPFD meter (Li-Cor LI-250A, Li-Cor Inc, NE, USA).

3.2 Gas exchange experiments

Gas exchange experiments were performed in an open system where a controlled flow of air enters and leaves the leaf cuvette, similar to the setup used by Pons and Welschen (2002). A schematic for the gas exchange experimental setup is shown in Fig. 2. The leaf cuvette had dimensions of $7 \times 7 \times 7\,cm^3$ ($l \times w \times h$) and the top part of the cuvette was transparent. The temperature of the leaf was measured with a K type thermocouple. The leaf chamber temperature was controlled by a temperature-controlled water bath kept at 20 °C (Tamson TLC 3, The Netherlands). A halogen lamp (Pradovit 253, Ernst Leitz Wetzlar GmbH, Germany) in a slide projector was used as a light source. Infrared was excluded by reflection from a cold mirror. The light intensity was varied with spectrally neutral filters (Pradovit 253, Ernst Leitz Wetzlar GmbH, Germany).

The CO_2 mole fraction of the incoming and outgoing air was measured with an infrared gas analyzer (IRGA, model LI-6262, Li-Cor Inc., NE, USA). The isotopic composition and mole fraction of the incoming and outgoing water vapor were measured with a triple water vapor isotope analyzer (WVIA, model 911-0034, Los Gatos Research, USA). Compressed air (ambient outside air without drying) was passed through soda lime to scrub the CO_2. The CO_2-free air could be humidified depending on the experiment conditions (see Fig. 2). The humidity of the inlet air was monitored continuously with a dew point meter (HYGRO-M1, General Eastern, Watertown, MA, USA). Pure CO_2 (either normal CO_2 or isotopically enriched CO_2) was mixed with the incoming air to produce a CO_2 mole fraction of 500 ppm. The isotopically enriched CO_2 was prepared by photochemical isotope exchange between CO_2 and O_2 under UV irradiation (Adnew et al., 2019).

An attached leaf or part of it was inserted into the cuvette, the composition of the inlet air was measured, and both IRGA and WVIA were switched to measure the outlet air. Based on the CO_2 mole fraction of the outgoing air the flow rate of the incoming air to the cuvette was adjusted to establish a drawdown of 100 ppm CO_2 due to photosynthesis in the plant chamber. The water vapor content entering the cuvette was adjusted depending on the transpiration rate relative to CO_2 uptake to avoid condensation (Fig. 2). The outgoing air was measured continuously until a steady state was reached for CO_2 and H_2O mole fractions and δD and $\delta^{18}O$ of the water vapor. After a steady state was established, the air was directed to the sampling flask while the IRGA and WVIA were switched back to measure the inlet air. The air

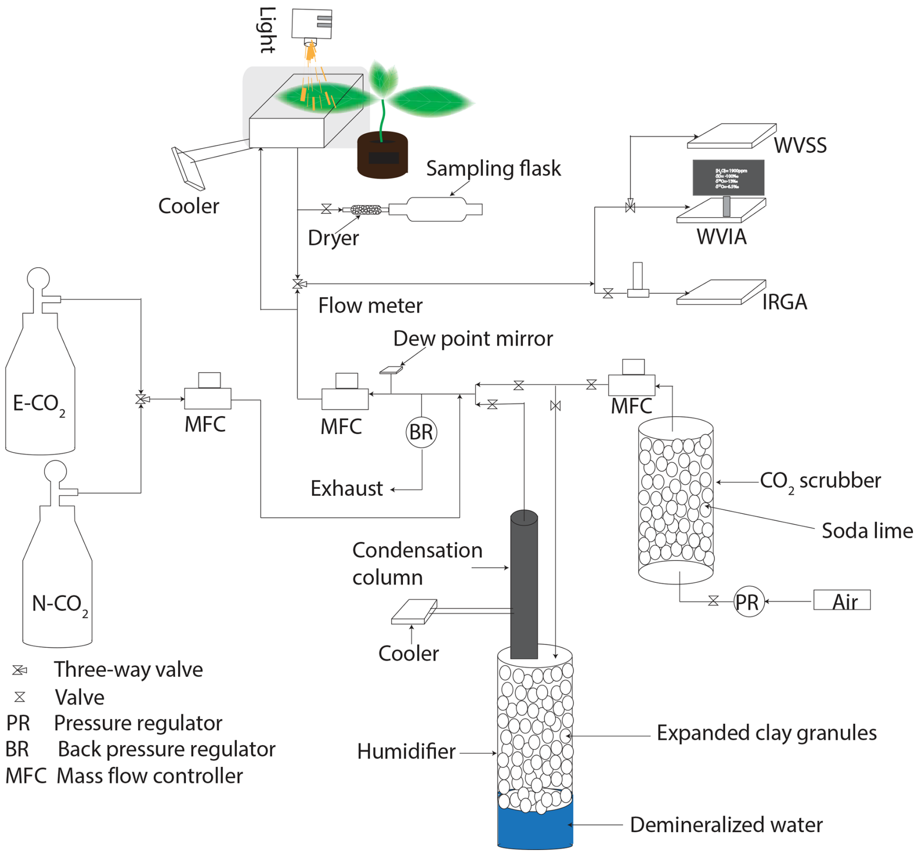

Figure 2. Schematic diagram of the leaf cuvette experimental setup. IRGA stands for the infrared gas analyzer, WVSS is the water vapor standard source, WVIA is the water vapor isotope analyzer, N-CO_2 is normal CO_2, and E-CO_2 is ^{17}O-enriched CO_2.

passed through a $Mg(ClO_4)_2$ dryer before entering the sampling flask.

After sampling, the leaf area inside the cuvette was measured with a LI-3100C area meter (Li-Cor Inc., USA). Immediately afterward, the leaf was placed in a leak-tight 9 mL glass vial and kept in a freezer at −20 °C until leaf water extraction.

3.3 Calibration of the water vapor isotope analyzer (WVIA) and leaf water analysis

The WVIA was calibrated using five water standards provided by IAEA (Wassenaar et al., 2018) for both $\delta^{18}O$ and δD (Fig. S2). We did not calibrate the WVIA for $\delta^{17}O$, so the $\delta^{17}O$ data are not used in the quantitative evaluation. The isotopic composition of the water standards ranged from −50.93 ‰ to 3.64 ‰ and −396.98 ‰ to 25.44 ‰ for $\delta^{18}O$ and δD, respectively. The detailed characterization and calibration of the WVIA is provided in the Supplement (Figs. S2 to S4).

Leaf water was extracted by cryogenic vacuum distillation for 4 h at 60 °C following a well-established procedure as shown in Fig. S5 (Wang and Yakir, 2000; Landais et al., 2006; West et al., 2006). Details are provided in the Supplement. The $\delta^{17}O$ and $\delta^{18}O$ of leaf water were determined at the Laboratoire des Sciences du Climat et de l'Environnement laboratory using a fluorination technique as described in Barkan and Luz (2005) and Landais et al. (2006, 2008).

3.4 Carbon dioxide extraction and isotope analysis

CO_2 was extracted from the air samples in a system made from electropolished stainless steel (Fig. S6). Our system used four commercial traps (MassTech, Bremen, Germany). The first two traps were operated at dry ice temperature (−78 °C) to remove moisture and some organics. The other two traps were operated at liquid nitrogen temperature (−196 °C) to trap CO_2. The flow rate during extraction was 55 mL min^{-1} controlled by a mass flow controller (Brooks Instruments, the Netherlands). The reproducibility of the extraction system was 0.030 ‰ for $\delta^{18}O$ and 0.007 ‰ for $\delta^{13}C$ determined on 14 extractions (1σ standard deviation, Table S1 in the Supplement).

The $\Delta^{17}O$ of CO_2 was determined using the CO_2–O_2 exchange method (Mahata et al., 2013; Barkan et al., 2015; Adnew et al., 2019). The CO_2–O_2 exchange system used at Utrecht University is described in Adnew et al. (2019). In short, equal amounts of CO_2 and O_2 were mixed in a quartz reactor containing a platinum sponge catalyst and heated at 750 °C for 2 h. After isotope equilibration, the CO_2 was trapped at liquid nitrogen temperature, while the O_2 was collected with 1 pellet of a 5Å molecular sieve (1.6 mm, Sigma Aldrich, USA) at liquid nitrogen temperature. The isotopic composition of the isotopically equilibrated O_2 was measured with a Delta^{Plus}XL isotope ratio mass spectrometer in dual-inlet mode with reference to a pure O_2 calibration gas that has been assigned values of $\delta^{17}O = 9.254$ ‰ and $\delta^{18}O = 18.542$ ‰ by Eugeni Barkan at the Hebrew University of Jerusalem. The reproducibility of the $\Delta^{17}O$ measurement was better than 0.01 ‰ (Table S1).

3.5 Leaf cuvette model

We used a simple leaf cuvette model to evaluate the dependence of $\Delta_A\Delta^{17}O$ on key parameters. In this model, the leaf is partitioned into three different compartments: the intercellular air space, the mesophyll cell, and the chloroplast. In the leaf cuvette model, we used a 100 ppm down-draw of CO_2, similar to the leaf exchange experiments, i.e., the CO_2 mole fraction decreases from 500 ppm in the entering air (c_e) to 400 ppm in the outgoing air (c_o), which is identical to the air surrounding the leaf (c_a) as a result of thorough mixing in the cuvette. The assimilation rate is set to 20.0 µmol m^{-2} s^{-1}. The leaf area and flow rate of air are set to 30 cm^2 and 0.7 L min^{-1}, respectively. The isotope composition of leaf water at the site where the H_2O-CO_2 exchange occurs is $\delta^{17}O = 5.39$ ‰ and $\delta^{18}O = 10.648$ ‰, which is the mean of the measured $\delta^{17}O$ and $\delta^{18}O$ values of bulk leaf water in our experiments. The leaf water temperature is set to 22 °C (similar to the experiment). In the model, the $\delta^{18}O$ of the CO_2 entering the cuvette is set to 30.47 ‰ for all the simulations, as in the normal CO_2 experiments, but the assigned $\Delta^{17}O$ values range from −0.5 ‰ to 0.5 ‰, which encompasses both the stratospheric intrusion and combustion components. The corresponding $\delta^{17}O$ of the CO_2 entering the cuvette is calculated from the assigned $\delta^{18}O$ value (30.47 ‰) and $\Delta^{17}O$ values (−0.5 ‰ to 0.5 ‰). For the calculations with this model, we assumed an infinite boundary layer conductance. The leaf cuvette model is illustrated in the Supplement (Fig. S7), and the detailed code and description is available at https://git.wur.nl/leaf_model (last access: 23 March 2020, Koren et al., 2020).

4 Results

4.1 Gas exchange parameters

Table 1 summarizes the isotopic composition and mole fraction of the CO_2 used in this study for sunflower, ivy and maize. The $\Delta^{17}O$ of CO_2 used in this study varies from −0.215 ‰ to 0.44 ‰, while the $\delta^{18}O$ value is close to 30 ‰ for all the experiments. For all the experiments, the mole fraction of CO_2 entering the leaf (c_a) is 400 ppm, whereas the mole fraction of the CO_2 in the intercellular air space (c_i), at the CO_2-H_2O exchange site (c_m), and in the chloroplast (c_c) varies depending on the assimilation rate and metabolism type of the plants. Estimating the mesophyll conductance is described in the companion paper. A detailed description for estimating c_m and c_c is provided in the Supplement. A list of variables and parameters used in this study are summarized in Table 2.

4.2 Discrimination against ^{18}O of CO_2

Figure 3a shows discrimination against ^{18}O associated with photosynthesis (Δ^{18}_AO) for sunflower, ivy, and maize as a function of the c_m/c_a ratio. Δ^{18}_AO varies with c_m/c_a, as found in previous studies (Gillon and Yakir, 2000a; Barbour et al., 2016) . For sunflower, we observe Δ^{18}_AO values between 29 ‰ and 64 ‰ for c_m/c_a between 0.54 and 0.86. Ivy shows relatively little variation in Δ^{18}_AO around a mean of 22 ‰ for c_m/c_a between 0.48 and 0.58. For maize, Δ^{18}_AO is lower than for the C_3 plants measured in this study, with values between 10 ‰ and 20 ‰ for c_m/c_a between 0.15 and 0.37.

For sunflower, changing the irradiance from 300 µmol m^{-2} s^{-1} (low light, hereafter LL) to 1200 µmol m^{-2} s^{-1} (high light, hereafter HL) leads to a clear decrease in Δ^{18}_AO (average 22 ‰). For maize, the Δ^{18}_AO change is only 4.4 ‰ on average. For ivy, changing the light intensity does not significantly change the observed Δ^{18}_AO. The solid lines in Fig. 3a show the results of leaf cuvette model calculations, where the dependence of Δ^{18}_AO on c_m/c_a is explored for a set of calculations with otherwise fixed parameters. The model agrees well with the experimental results, except for ivy, where the model overestimates the discrimination.

4.3 Discrimination against $\Delta^{17}O$ of CO_2

The discrimination of photosynthesis against $\Delta^{17}O$ of CO_2 ($\Delta_A\Delta^{17}O$) is shown in Fig. 3b. $\Delta_A\Delta^{17}O$ is negative for all experiments, it depends strongly on the c_m/c_a ratio, and $|\Delta_A\Delta^{17}O|$ increases with c_m/c_a ratio. For instance, for $\Delta^{17}O$ of CO_2 entering the cuvette of −0.215 ‰, $\Delta_A\Delta^{17}O$ is −0.25 ‰ for maize with c_m/c_a ratio of 0.3, −0.3 ‰ for ivy with c_m/c_a ratio of 0.5 ‰, and −0.5 ‰ for sunflower with c_m/c_a ratio of 0.7 (Fig. 3b). For sunflower and ivy, $\Delta_A\Delta^{17}O$ is also strongly dependent on the $\Delta^{17}O$ of CO_2 supplied to the cuvette, whereas no significant dependence is found for maize. For an increase in $\Delta^{17}O$ of CO_2 entering the cuvette from −0.215 ‰ to 0.435 ‰, $\Delta_A\Delta^{17}O$ increases from −0.3 ‰ to −0.9 ‰ at c_m/c_a ratio of 0.5 for ivy. For sunflower, an increases $\Delta^{17}O$ of CO_2 entering the cuvette from −0.215 ‰ to 0.31 ‰ increases $\Delta_A\Delta^{17}O$ from −0.8 ‰ to −1.7 ‰ at c_m/c_a ratio of 0.8. The leaf cuvette model results illustrate the shape of the dependence on the c_m/c_a ratio and agree well with the experiments. For the leaf cuvette model,

Table 1. Summary of gas exchange parameters and isotopic compositions of maize, sunflower, and ivy. Mole fraction at the site of exchange (c_m) is calculated assuming complete isotopic equilibrium with the water at the CO_2-H_2O exchange site. The water at the CO_2-H_2O exchange site is assumed to be the same as the isotopic composition at the site of evaporation. Numbers in parentheses are the standard deviations of the mean (1σ).

Parameter	Unit	Sunflower	Ivy	Maize	Irradiance ($\mu mol\,m^{-2}\,s^{-1}$)
A_n	$\mu mol\,mol^{-1}\,m^{-2}\,s^{-1}$	18 (0.7)	12 (0.7)	17 (2)	300
		29 (2)	15 (2)	32 (2)	1200
g_s	$mol\,m^{-2}\,s^{-1}$	0.45 (0.14)	0.11 (0.02)	0.08 (0.01)	300
		0.40 (0.04)	0.15 (0.03)	0.16 (0.02)	1200
$\delta^{18}O_e$	‰	27.26 to 31.80	28.28 to 30.48	27.26 to 30.48	
$\Delta^{17}O_e$	‰	−0.227 to 0.409	−0.215 to 0.435	−0.215 to 0.310	
$\delta^{18}O_a$	‰	33.25 to 43.87	32.64 to 35.86	34.04 to 29.764	
$\Delta^{17}O_a$	‰	−0.333 to 0.163	−0.276 to 0.327	−0.270 to 0.296	
$\Delta^{18}_A O_{obs}$	‰	57.12 (4.70)	22.20 (1.32)	17.23 (1.32)	300
		34.48 (3.25)	24.35 (3.09)	12.78 (0.83)	1200
$\Delta_A\Delta^{17}O_{obs}$	‰	−2.61 to −0.43	−1.03 to −0.19	−0.36 to −0.09	
$\delta^{18}O_m$	‰	52.02 (1.24)	47.17 (1.17)	52.62 (0.52)	300
		52.62 (1.42)	51.09 (1.76)	55.15 (1.55)	1200
$\Delta^{17}O_m$	‰	−0.41(0.001)	−0.35(0.001)	−0.40(0.01)	300
		−0.41(0.01)	−0.38(0.02)	−0.42(0.02)	1200
c_a	ppm	402 (3)	403 (3)	403 (3)	
c_i	ppm	357 (10)	284 (0.1)	194 (20)	300
		323 (10)	301 (13)	194 (15)	1200
c_c	ppm	277 (15)	188 (30)		300
		201 (42)	163 (21)		1200
c_m	ppm	320 (10)	220 (10)	134 (15)	300
		252 (27)	214 (12)	88 (17)	1200

the $\Delta^{17}O$ value of the water is assigned a constant value of −0.122 ‰ (average $\Delta^{17}O$ value for the bulk leaf water).

Figure 4b shows the same values of $\Delta_A\Delta^{17}O$ as a function of the difference between $\Delta^{17}O$ of CO_2 entering the leaf and the calculated $\Delta^{17}O$ of leaf water at the evaporation site where CO_2-H_2O exchange takes place ($\Delta^{17}O_a-\Delta^{17}O_{wes}$) for different c_m/c_a ratios. The leaf cuvette model results (solid lines in Fig. 4b) suggest a linear dependence between $\Delta_A\Delta^{17}O$ and ($\Delta^{17}O_a-\Delta^{17}O_{wes}$). The experimental results agree with the hypothesis that $\Delta_A\Delta^{17}O$ is linearly dependent on $\Delta^{17}O_a-\Delta^{17}O_{wes}$ at a certain c_m/c_a ratio. Figure 4a shows the corresponding relation where $\Delta_A\Delta^{17}O$ is divided by $\Delta^{17}O_a-\Delta^{17}O_m$. All the values follow the same relationship as a function of the c_m/c_a ratio, which can be approximated quite well by an exponential function (Eq. 5). This function quantifies the dependence of $\Delta_A\Delta^{17}O$ on c_m/c_a and thus the effect of the diffusion of isotopically exchanged CO_2 back to the atmosphere, which increases with increasing c_m/c_a ratio.

$$\frac{\Delta_A\Delta^{17}O}{\Delta^{17}O_a-\Delta^{17}O_m} = -0.150 \times \exp(3.707 \times c_m/c_a) + 0.028 \quad (5)$$

Figure 5a and c show results from the leaf cuvette model that illustrates in more detail how $\Delta^{17}O_e$ and $\Delta^{17}O_{wes}$ affect $\Delta^{17}O_a$ and $\Delta_A\Delta^{17}O$ and their dependence on c_m/c_a. At lower c_m/c_a, only a very small fraction of CO_2 that has undergone isotopic equilibration in the mesophyll diffuses back to the atmosphere, and therefore $\Delta^{17}O_a$ stays close to

Table 2. List of symbols and variables.

Symbol	Description	Unit/calculation/value
Gas exchange		
A_n	Rate of CO_2 assimilation	$\frac{u_e}{s}\left(c_e - c_a\left(\frac{1-w_e}{1-w_a}\right)\right)$, mol m^{-2} s^{-2}
E	Transpiration rate	$\frac{u_e}{s}\left(\frac{w_a-w_e}{1-w_a}\right)$, mol m^{-2} s^{-2}
w_i	Mole fraction of water vapor inside leaf	$\frac{613.65\times e^{\left(\frac{17.502\times T_{leaf}}{240.97+T_{leaf}}\right)}\times 10^{-5}}{P}$, mol mol^{-1}
w_a	Mole fraction of water vapor leaving the cuvette or leaf surrounding	mol mol^{-1}
w_e	Mole fraction of water vapor entering the cuvette	mol mol^{-1}
c_e	Mole fraction of CO_2 entering the cuvette	mol mol^{-1}
c_a	Mole fraction of CO_2 in the leaf surrounding or leaving the cuvette	mol mol^{-1}
u_e	Flow rate of air entering the cuvette	mol s^{-1}
s	Surface area of the leaf inside the cuvette	m^{-2}
P	Atmospheric pressure	bar
T_{leaf}	Leaf temperature	°C
$g_{s(H2O)}$	Stomatal conductance for water vapor	$\frac{g^t_{H_2O}\times g_{b(H_2O)}}{g_{b(H_2O)}-g^t_{H_2O}}$
$g_{b(H2O)}$	Boundary layer conductance for water vapor	Calibrated for the cuvette we used
$g^t_{H_2O}$	Conductance for water vapor through the boundary layer and stomata	$E\left(\frac{1-\left(\frac{w_i+w_a}{2}\right)}{w_i-w_a}\right)$, mol m^{-2} s^{-1}
g_s	Stomatal conductance for CO_2	$\frac{g_{s(H_2O)}}{1.6}$
g_b	Boundary conductance for CO_2	$\frac{g_{b(H_2O)}}{1.37}$
$g^t_{CO_2}$	Conductance for CO_2 through the boundary layer and stomata	$\frac{g_s\times g_b}{g_s+g_b}$
Γ^*	CO_2 compensation point	45 µmol m^{-2} s^{-1}
g_{m13}	CO_2 conductance from intercellular air space to the site of carboxylation calculated using $\Delta^{13}_A C$ (for C_3 plants only)	mol m^{-2} s^{-1} bar^{-1}
g_{m18}	CO_2 conductance from intercellular air space to CO_2-H_2O exchange site calculated using $\Delta^{18}_A O$	mol m^{-2} s^{-1} bar^{-1}
g_{m17}	CO_2 conductance from intercellular air space to CO_2-H_2O exchange site calculated using $\Delta^{17}_A O$	mol m^{-2} s^{-1} bar^{-1}
$g_{m\Delta17}$	CO_2 conductance from intercellular air space to CO_2-H_2O exchange site calculated using $\Delta_A\Delta^{17}O$	mol m^{-2} s^{-1} bar^{-1}
c_i	Mole fraction of CO_2 in the intercellular air space	$\frac{\left(g^t_{CO_2}-\frac{E}{2}\right)c_a-A_n}{\left(g^t_{CO_2}+\frac{E}{2}\right)}$ mol mol^{-1}
c_s	Mole fraction of CO_2 at the leaf surface	$c_a-\frac{A_n}{g_b}$
c_m	Mole fraction of CO_2 at the site of CO_2-H_2O exchange	mol mol^{-1}
c_c	Mesophyll conductance to the chloroplast (for C_3 plants)	$c_i-\frac{A_n}{g_{m13}}$ mol mol^{-1}
t^{13}	Ternary correction for $^{13}CO_2$	$\frac{(1+a_{13bs})E}{2g^t_{CO_2}}$
t^{18}	Ternary correction for $C^{18}OO$	$\frac{(1+a_{18bs})E}{2g^t_{CO_2}}$
t^{17}	Ternary correction for $C^{17}OO$	$\frac{(1+a_{17bs})E}{2g^t_{CO_2}}$
R_D	Dark respiration rate	0.8 µmol m^{-2} s^{-1}
R_L	Day respiration rate	$0.5\times R_D$ µmol m^{-2} s^{-1}

Table 2. Continued.

Symbol	Description	Unit/calculation/value
Oxygen and carbon isotope effects		
ε_k^{18}	Kinetic fractionation of water vapor in air	$\frac{28g_b+19g_s}{g_b+g_s}$, ‰
ε_{equ}^{18}	Equilibrium fractionation between liquid and gas phase of water vapor	$2.644-3.206\left(\frac{10^3}{T_{leaf}}\right)+1.534\left(\frac{10^6}{T_{leaf}}\right)$, ‰
a_{13bs}	Weighted fractionation for ^{13}COO as CO_2 diffuses through the boundary layer and stomata	$\frac{(c_s-c_i)a_{13s}+(c_a-c_s)a_{13b}}{c_a-c_i}$, ‰
a_{17bs}	Weighted fractionation for $C^{17}OO$ as CO_2 diffuses through the boundary layer and stomata	$\frac{(c_s-c_i)a_{17s}+(c_a-c_s)a_{17b}}{c_a-c_i}$, ‰
a_{18bs}	Weighted fractionation for $C^{18}OO$ as CO_2 diffuses through the boundary layer and stomata	$\frac{(c_s-c_i)a_{18s}+(c_a-c_s)a_{18b}}{c_a-c_i}$, ‰
a_{13bs}	Weighted fractionation for ^{13}COO as CO_2 diffuses through the boundary layer and stomata	$\frac{(c_s-c_i)a_{13s}+(c_a-c_s)a_{13b}}{c_a-c_i}$ ‰
a_{18bs}	Weighted fractionation for $C^{18}OO$ as CO_2 diffuses through the boundary layer and stomata	$\frac{(c_s-c_i)a_{18s}+(c_a-c_s)a_{18b}}{c_a-c_i}$, ‰
a_{17bs}	Weighted fractionation for $C^{17}OO$ as CO_2 diffuses through the boundary layer and stomata	$\frac{(c_s-c_i)a_{17s}+(c_a-c_s)a_{17b}}{c_a-c_i}$ ‰
$\overline{a}_{17}$	Weighted fractionation of $C^{17}OO$ as it diffuses through the boundary layer, stomata, and liquid phase in series	$\frac{(c_i-c_m)a_{17w}+(c_s-c_i)a_{17s}+(c_a-c_s)a_{17b}}{c_a-c_m}$, ‰
$\overline{a}_{18}$	Weighted fractionation of $C^{18}OO$ as it diffuses through the boundary layer, stomata, and liquid phase in series	$\frac{(c_i-c_m)a_{18w}+(c_s-c_i)a_{18s}+(c_a-c_s)a_{18b}}{c_a-c_m}$, ‰
a_{13b}	Fractionation in $^{13}CO_2$ as CO_2 diffuses through the boundary layer	2.9 ‰
a_{13s}	Fractionation in $^{13}CO_2$ as CO_2 diffuses through the stomata	4.4 ‰
a_m	Fractionation factor for dissolution and diffusion through water	1.8 ‰
f	Fractionation factor for photorespiration (decarboxylation of glycine)	16 ‰
e	Fractionation factor for day respiration	R_D+e^*, ‰
$e*$	Apparent fractionation for day respiration	$\delta^{13}C_a-\Delta_A^{13}C-\delta^{13}C_{substrate}$, ‰
b	Fractionation factor for uptake by RuBisCO	29 ‰
α_f	Fractionation due to photorespiration (decarboxylation of glycine)	$1+f$
α_e	Fractionation due to day respiration	$1+e$
α_b	Fractionation due to uptake by RuBisCO	$1+b$
a_{17b}	Fractionation of $C^{17}OO$ as CO_2 diffuses through the boundary layer	2.9 ‰
a_{17s}	Fractionation in $C^{17}OO$ as CO_2 diffuses through stomata	4.4 ‰
a_{18b}	Fractionation of $C^{18}OO$ as CO_2 diffuses through the boundary layer	5.8 ‰
a_{18s}	Fractionation in $C^{18}OO$ as CO_2 diffuses through stomata	8.8 ‰
a_{17w}	Fractionation in $C^{17}OO$ due to diffusion and dissolution in water	0.382 ‰
a_{18w}	Fractionation in $C^{18}OO$ due to diffusion and dissolution in water	0.8 ‰
ε_W^{18}	Equilibrium fractionation of CO_2 and water for $C^{18}OO$	$\frac{17\,604}{T_{leaf}}-17.93$, ‰
ε_k^{18}	kinetic fractionation of water vapor in air	$\frac{28\times g_b+19\times g_s}{g_b+g_s}$
ε_{equ}^{18}	equilibrium fractionation between liquid- and gas-phase water	$2.644-3.206\times\left(\frac{10^3}{T}\right)+1.534\times\left(\frac{10^6}{T}\right)$

Table 2. Continued.

Symbol	Description	Unit/calculation/value
Isotopic composition		
$\delta^{17}O_A$	$\delta^{17}O$ of the assimilated CO_2	$\frac{\delta^{17}O_a-\Delta^{17}_AO}{\Delta^{17}_AO+1}=\delta^{17}O_a-\frac{c_e}{c_e-c_a}\left(\delta^{17}O_a-\delta^{17}O_e\right)$
$\delta^{18}O_A$	$\delta^{18}O$ of the assimilated CO_2	$\frac{\delta^{18}O_a-\Delta^{18}_AO}{\Delta^{18}_AO+1}=\delta^{18}O_a-\frac{c_e}{c_e-c_a}\left(\delta^{18}O_a-\delta^{18}O_e\right)$
$\delta^{17}O_{io}$	$\delta^{17}O$ of CO_2 in the intercellular air space ignoring ternary correction	$\delta^{17}O_A\left(1-\frac{c_a}{c_i}\right)(1+a_{17bs})+\frac{c_a}{c_i}\left(\delta^{17}O_a-a_{17bs}\right)+a_{17bs}$, ‰
$\delta^{18}O_{io}$	$\delta^{18}O$ of CO_2 in the intercellular air space ignoring ternary correction	$\delta^{18}O_A\left(1-\frac{c_a}{c_i}\right)(1+a_{18bs})+\frac{c_a}{c_i}\left(\delta^{18}O_a-a_{18bs}\right)+a_{18bs}$, ‰
$\delta^{17}O_i$	$\delta^{17}O$ of CO_2 in the intercellular air space	$\frac{\delta^{17}O_{io}+t^{17}\left(\delta^{17}O_A\left(\frac{c_a}{c_i}+1\right)-{}^{17}O_a\frac{c_a}{c_i}\right)}{1+t^{17}}$, ‰
$\delta^{18}O_i$	$\delta^{18}O$ of CO_2 in the intercellular air space	$\frac{\delta^{18}O_{io}+t^{18}\left(\delta^{18}O_A\left(\frac{c_a}{c_i}+1\right)-{}^{18}O_a\frac{c_a}{c_i}\right)}{1+t^{18}}$, ‰
$\delta^{18}O_{trans}$	$\delta^{18}O$ of transpired water vapor	$\left(\frac{w_a}{w_a-w_e}\right)\left(\delta^{18}O_{wa}-\delta^{18}O_{we}\right)+\delta^{18}O_{we}$, ‰
$\delta^{18}O_{wes}$	$\delta^{18}O$ of water at the evaporation site	$\delta^{18}O_{wes}=\delta^{18}O_{trans}+\varepsilon^{18}_k+\varepsilon^{18}_{equ}+\frac{w_a}{w_i}\times\left(\delta^{18}O_{wa}-\varepsilon^{18}_k+\delta^{18}O_{trans}\right)$
$\delta^{17}O_m$	$\delta^{17}O$ of CO_2 at the site of CO_2-H_2O exchange	$\left(\delta^{17}O_{wes}+1\right)\times\left(1+\varepsilon^{17}_w\right)-1$, ‰
$\delta^{18}O_m$	$\delta^{18}O$ of CO_2 at the site of CO_2-H_2O exchange	$\left(\delta^{18}O_{wes}+1\right)\times\left(1+\varepsilon^{18}_w\right)-1$, ‰
$\delta^{13}C_{substrate}$	Isotope (^{13}C) ratio of substrate used for dark respiration	$\frac{\delta^{13}C_a-\Delta^{13}_AC}{\Delta^{13}_AC+1}$, ‰
Δ^{13}_AC	^{13}C-photosynthetic discrimination	$\frac{\zeta\left(\delta^{13}C_a-\delta^{13}C_e\right)}{1+\delta^{13}C_a-\left(\delta^{13}C_a-\delta^{13}C_e\right)}$, ‰
$\Delta^{13}_AC_{obs}$	^{13}C-photosynthetic discrimination (Farquhar model)	$\left(\frac{1}{1-t}\right)\left[a_{13bs}\frac{c_a-c_i}{c_a}\right]+\left(\frac{1+t}{1-t}\right)\left[a_m\frac{c_i-c_c}{c_a}+b\frac{c_c}{c_a}-\frac{\alpha_b}{\alpha_e}e\frac{R_D}{R_D+A_n}\frac{c_c-\Gamma^*}{c_a}-\frac{\alpha_b}{\alpha_f}f\frac{\Gamma^*}{c_a}\right]$
$\Delta^{13}_AC_i$	^{13}C-photosynthetic discrimination (assuming no mesophyll conductance, i.e., $c_i=c_c$)	$\left(\frac{1}{1-t}\right)\left[\overline{a}\frac{c_a-c_i}{c_a}\right]+\left(\frac{1+t}{1-t}\right)\left[b\frac{c_i}{c_a}-\frac{\alpha_b}{\alpha_e}e\frac{R_D}{R_D+A_n}\frac{c_i-\Gamma^*}{c_a}-\frac{\alpha_b}{\alpha_f}f\frac{\Gamma^*}{c_a}\right]$
Δ^{18}_AO	^{18}O-photosynthetic discrimination	$\frac{\zeta\left(\delta^{18}O_a-\delta^{18}O_e\right)}{1+\delta^{18}O_a-\zeta\left(\delta^{18}O_a-\delta^{18}O_e\right)}$, ‰
Δ^{17}_AO	^{17}O-photosynthetic discrimination	$\frac{\zeta\left(\delta^{17}O_a-\delta^{17}O_e\right)}{1+\delta^{17}O_a-\zeta\left(\delta^{17}O_a-\delta^{17}O_e\right)}$, ‰
$\Delta^{17}_AO_{FM}$	Farquhar model for ^{17}O-photosynthetic discrimination	$\frac{\overline{a}_{17}+\frac{c_m}{c_a-c_m}\delta^{17}O_{ma}}{1-\frac{c_m}{a-c_m}\delta^{17}O_{ma}}$, ‰
$\Delta^{18}_AO_{FM}$	Farquhar model for ^{18}O-photosynthetic discrimination	$\frac{\overline{a}_{18}+\frac{c_m}{c_a-c_m}\delta^{18}O_{ma}}{1-\frac{c_m}{c_a-c_m}\delta^{18}O_{ma}}$, ‰
$\delta^{17}O_e$	$\delta^{17}O$ of CO_2 entering the cuvette	‰
$\delta^{17}O_a$	$\delta^{17}O$ of CO_2 leaving the cuvette	‰
$\delta^{18}O_e$	$\delta^{18}O$ of CO_2 entering the cuvette	‰
$\delta^{18}O_a$	$\delta^{18}O$ of CO_2 leaving the cuvette	‰
$\delta^{17}O_{ma}$	$\delta^{17}O$ of CO_2 equilibrated with the leaf water at the evaporating site relative to the CO_2 leaving the cuvette	$\frac{\delta^{17}O_m-\delta^{17}O_a}{1-\delta^{18}O_a}$, ‰
$\delta^{18}O_{ma}$	$\delta^{18}O$ of CO_2 equilibrated with the leaf water at the evaporating site relative to the CO_2 leaving the cuvette	$\frac{\delta^{18}O_m-\delta^{18}O_a}{1-\delta^{18}O_a}$, ‰
$\delta^{18}O_{we}$	$\delta^{18}O$ of water vapor entering the cuvette	‰
$\delta^{18}O_{wa}$	$\delta^{18}O$ of water vapor leaving the cuvette or leaf surrounding	‰

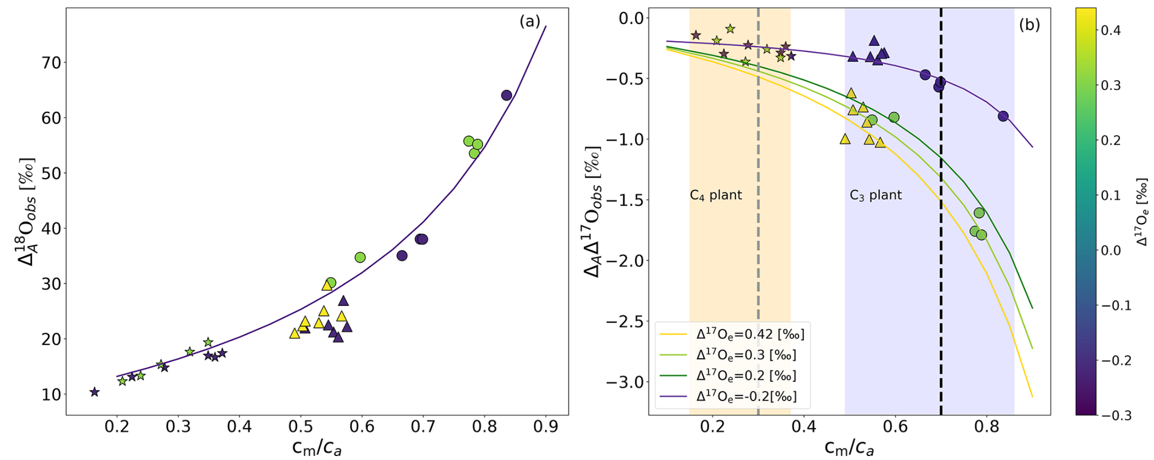

Figure 3. (a) $\Delta^{18}_{A}O_{obs}$ during photosynthesis for two C_3 plants, sunflower (circles) and ivy (triangles), and C_4 plant maize (stars), as a function of c_m/c_a. The solid lines show results from the leaf cuvette model, where $\delta^{18}O$ of the CO_2 entering the cuvette is 30.47 ‰. **(b)** $\Delta_A\Delta^{17}O$ of CO_2 as a function of c_m/c_a for isotopically different CO_2 gases entering the cuvette (color bar shows $\Delta^{17}O_e$) for sunflower (circles), ivy (triangles), and maize (stars). $\Delta_A\Delta^{17}O$ values calculated using the leaf cuvette model are shown as solid lines in corresponding colors ($\Delta^{17}O_e$ values are given in the legend). The shaded areas indicate the c_m/c_a ranges for C_4 and C_3 plants, and the vertical dashed lines indicate the mean c_m/c_a ratio used for extrapolating from the leaf scale to the global scale. The solid line is the leaf cuvette model results for the corresponding c_m/c_a ratio.

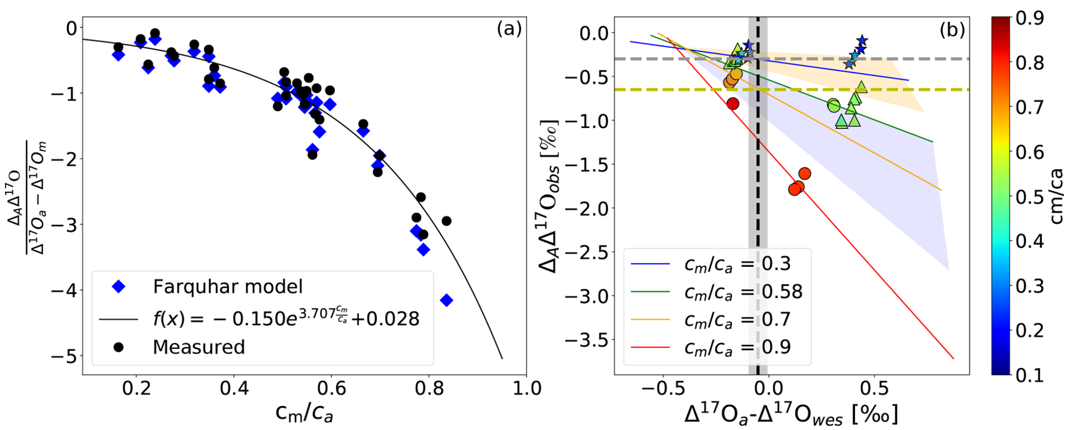

Figure 4. (a) Dependency of $\Delta_A\Delta^{17}O$ on the relative difference of the $\Delta^{17}O(CO_2)$ entering the leaf and the $\Delta^{17}O$ of CO_2 in equilibrium with leaf water against the c_m/c_a ratio. **(b)** Dependency of $\Delta_A\Delta^{17}O$ on the difference between the $\Delta^{17}O$ of CO_2 entering the cuvette and the $\Delta^{17}O$ of leaf water at the evaporation site color coded for different c_m/c_a ratios. The solid lines are the results of the leaf cuvette model for different c_m/c_a ratios as stated in the legend. The vertical dashed black line indicates the difference between the global average $\Delta^{17}O$ value for CO_2 (−0.168 ‰) and leaf water (−0.067 ‰) (Koren et al., 2019). The gray and yellow horizontal dashed lines indicate global $\Delta_A\Delta^{17}O$ of C_4 and C_3 plants for a c_m/c_a ratio of 0.3 and 0.7, respectively.

the incoming $\Delta^{17}O_e$, modified by the fractionation during CO_2 diffusion through the stomata (Fig. 5a). Figure 5c confirms that at low c_m/c_a, $\Delta_A\Delta^{17}O$ approaches the fractionation constant expected for diffusion, −0.170 ‰. This diffusional fractionation is independent of the isotopic composition of the CO_2 entering the leaf, and therefore at low c_m/c_a, the $\Delta_A\Delta^{17}O$ curves for the different values of the anomaly of the CO_2 entering the leaf converge. For a high c_m/c_a ratio, the back-diffusion flux of CO_2 that has equilibrated with water becomes the dominant factor, and, in this case, the isotopic composition of the outgoing CO_2 converges towards this isotope value, independent of the isotopic composition of the incoming CO_2 (Fig. 5a). This can lead to a very wide range of values for the discrimination against $\Delta^{17}O$ because now the effect on $\Delta^{17}O$ of the ambient CO_2 depends strongly on the difference in isotopic composition between incoming CO_2 and CO_2 in isotopic equilibrium with the leaf water.

In the model calculations shown in Fig. 5b and d, the isotopic composition of the water was changed from $\Delta^{17}O_{wes}$ = −0.122 ‰ to 0.300 ‰, whereas all other parameters were

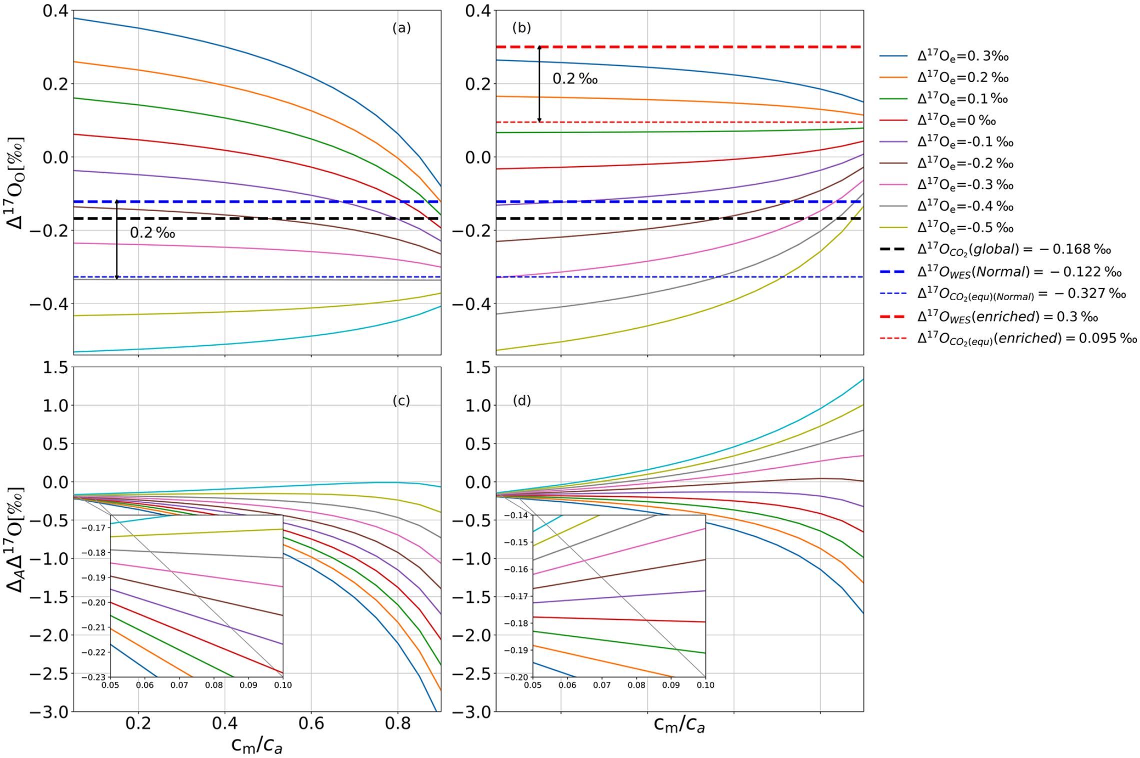

Figure 5. **(a, b)** $\Delta^{17}O_a$ as a function of c_m/c_a for various values of $\Delta^{17}O_e$ (see legend) for $\Delta^{17}O_{wes} = -0.122$ ‰ in **(a)** and $\Delta^{17}O_{wes} = 0.300$ ‰ in **(b)**. Panels **(c, d)** show the corresponding values for $\Delta_A\Delta^{17}O$. $\Delta^{17}O_{global}$ is the global average $\Delta^{17}O$ value for atmospheric CO_2 (Koren et al., 2019). When $\Delta^{17}O$ of CO_2 entering the cuvette is approximately 0.2 ‰ lower than the $\Delta^{17}O$ of leaf water at the CO_2-H_2O exchange site, $\Delta^{17}O$ of the CO_2 leaving the cuvette does not change when the c_m/c_a ratio varies.

kept the same. The value of $\Delta^{17}O_e$ for which $\Delta^{17}O_a$ does not depend on c_m/c_a is shifted accordingly, again being similar to $\Delta^{17}O_m$. At low c_m/c_a, $\Delta_A\Delta^{17}O$ converges to the same value as in Fig. 5c, confirming the role of diffusion into the stomata as discussed above.

Figure 6 shows how $\delta^{18}O$ and $\Delta^{17}O$ vary in key compartments of the leaf cuvette system that determine the oxygen isotope effects associated with photosynthesis, based on the previously established three-isotope slopes of the various processes (Fig. 1). The irrigation water has a $\Delta^{17}O$ value of 0.017 ‰. The measured bulk leaf water is 6 ‰ to 16 ‰ enriched in ^{18}O and its $\Delta^{17}O$ value is lower by −0.075 ‰ to −0.200 ‰ (mean value −0.121 ‰) than the irrigation water, calculated using a three-isotope slope of $\theta_{trans} = 0.516$ % at 80 % humidity (Landais et al., 2006). $\Delta^{17}O$ of leaf water at the evaporation site, calculated from the transpired water, has slightly lower $\Delta^{17}O$, with values between −0.119 ‰ and −0.237 (average −0.184 ‰). Note that the bulk leaf water was not measured for all the experiments. For the experiments where the bulk leaf water is measured, $\Delta^{17}O$ of leaf water at the evaporation site ranges from −0.160 ‰ to −0.231 ‰ with an average value of -0.190 ± 0.020 ‰. The calculated isotopic composition of water at the exchange site was thus similar but slightly lower in $\Delta^{17}O$ than the values measured for bulk leaf water. CO_2 exchanges with the water in the leaf with a well-established fractionation constant (see Eq. S17) and a three-isotope slope of $\theta_{CO_2-H_2O} = 0.5229$ (Barkan and Luz, 2012), leading to the lower $\Delta^{17}O$ values of the equilibrated CO_2. In our experiments, the $\Delta^{17}O$ value of CO_2 in equilibrium with leaf water is lower than the $\Delta^{17}O$ value of CO_2 entering the leaf. The $\Delta^{17}O$ of the CO_2 in the intercellular air space is a mixture between two end-members, the $\Delta^{17}O$ of the CO_2 entering the leaf and $\Delta^{17}O$ of the CO_2 in equilibrium with leaf water. This explains why the observed values of $\Delta_A\Delta^{17}O$ are negative for the experiments performed in this study.

5 Discussion

5.1 Discrimination against $\delta^{18}O$ of CO_2

The higher $\Delta^{18}_AO_{obs}$ values for sunflower compared to maize and ivy (Fig. 3a) are mainly due to a higher back-diffusion flux ($c_m/(c_a - c_m)$). The back-diffusion flux is higher for the C_3 plants sunflower and ivy than for the C_4 plant maize, a consequence of the lower stomatal conductance and higher assimilation rate of C_4 plants (Gillon and Yakir, 2000a; Barbour et al., 2016). In C_4 plants most of the CO_2 entering

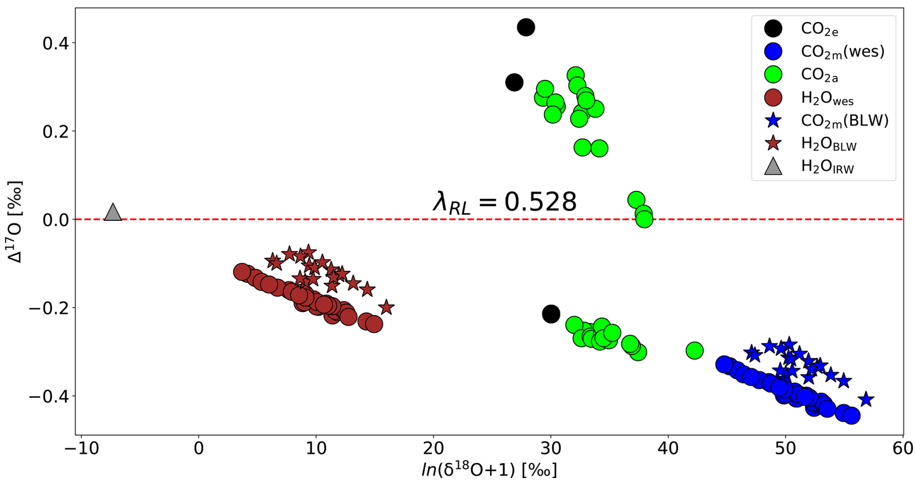

Figure 6. Isotopic composition of various relevant oxygen reservoirs that affect the $\Delta^{17}O$ of atmospheric CO_2 during photosynthesis: irrigation water (gray triangle), calculated leaf water at the evaporation site (brown circles), measured bulk leaf water (brown star), CO_2 entering the cuvette (black circles), CO_2 leaving the leaf cuvette (green circles), CO_2 equilibrated with leaf water at the evaporation site (blue circles), and CO_2 equilibrated with bulk leaf water (blue stars). $\Delta^{17}O$ is calculated with $\lambda = 0.528$.

the stomata is carboxylated by phosphoenolpyruvate carboxylase (PEPC), resulting in a lower CO_2 mixing ratio in the mesophyll, which results in a lower back-diffusion flux. The increase in assimilation rate with higher light intensity decreases the c_m/c_a ratio and thus leads to a lower back-diffusion flux, which explains the decreases in $\Delta^{18}_A O_{obs}$ for maize and most clearly for sunflower. A similar trend of increase in $\Delta^{18}_A O_{obs}$ with an increase in c_m/c_a ratio has been reported in previous studies (Gillon and Yakir, 2000b, a; Osborn et al., 2017). For ivy, $\Delta^{18}_A O_{obs}$ and $\Delta^{17}_A O_{obs}$ do not decrease with an increase in irradiance because the change in assimilation rate with irradiance is small. Thus, c_m will not decrease strongly and the effect on the back diffusion is smaller than the variability in $\Delta^{18}_A O_{obs}$ of different leaves of the same plant.

In our experiments, photosynthesis causes an enrichment in the $\delta^{18}O$ of atmospheric CO_2 for both C_3 and C_4 plants, i.e., positive value of $\Delta^{18}_A O$. In principle, $\Delta^{18}_A O$ can also be negative if the $\delta^{18}O_m$ is depleted relative to the ambient CO_2. This is in contrast to $\Delta^{13}_A C$, which will always be positive since it is determined by the fractionation due to the PEPC and RuBisCO enzyme activity (Figs. S8 and S9). In general, in our experiments the $\Delta^{18}_A O_{obs}$ values are about 5 times larger than $\delta^{18}O_a - \delta^{18}O_e$, the $\delta^{18}O$ difference between CO_2 entering and leaving the cuvette (Figs. S10 to S12). This is easy to understand from the definition of Δ_A. Taking $\Delta^{18}_A O$ as an example, $\Delta^{18}_A O_{obs} = \frac{\zeta(\delta^{18}O_a - \delta^{18}O_e)}{1+\delta^{18}O_a - \zeta(\delta^{18}O_a - \delta^{18}O_e)} \approx \left(\delta^{18}O_a - \delta^{18}O_e\right)$, and in our experiments $\zeta = c_e/(c_e - c_a) \approx 500/(500-400) = 5$.

5.2 Discrimination against the $\Delta^{17}O$ of CO_2

The leaf cuvette model includes the isotope fractionations of all the individual processes that have been quantified in dedicated experiments previously (Fig. 1). The good agreement of the model results with the measurements (Fig. 3a) demonstrates that when all these processes are combined in the quantitative description of a gas exchange experiment, they actually result in a correct quantification of the isotope effects associated with photosynthesis. This has already been demonstrated before for $\Delta^{18}_A O_{obs}$ but has now been confirmed for $\Delta_A \Delta^{17}O$.

Unlike ivy and sunflower, maize does not show a significant change in $\Delta_A \Delta^{17}O$ when CO_2 gases with different $\Delta^{17}O$ are supplied to the plant. The C_4 plant maize has a small back-diffusion flux due to its high assimilation rate and low stomatal conductance, leading to a low c_m/c_a ratio. At low c_m/c_a ratios, $\Delta_A \Delta^{17}O$ is expected to be close to the weighted fractionation due to diffusion through boundary layer and stomata. In general, the effect of diffusion on $\Delta^{17}O$ of atmospheric CO_2 can be expressed as follows:

$$\Delta^{17}O_{Modified} = \Delta^{17}O_a + \left(\lambda_{RL} - \theta_{CO_2-diff}\right) \times \ln \alpha_{diffusion}, \quad (6)$$

where $\Delta^{17}O_a$ is the $\Delta^{17}O$ of the CO_2 surrounding the leaf; $\Delta^{17}O_{modified}$ is the $\Delta^{17}O$ of the CO_2 modified due to diffusional fractionation; and θ_{CO_2-diff}, λ_{RL}, and $\alpha_{diffusion}$ are the oxygen three-isotope relationships during diffusion from the CO_2-H_2O exchange site to the atmosphere, the reference slope used, and the fractionation against ^{18}O for CO_2 during diffusion through the stomata. Using the values $\lambda_{RL} = 0.528$, $\theta_{CO_2-diff} = 0.509$ (Young et al., 2002), and $\alpha_{diffusion} = 0.9912$ (Farquhar and Lloyd, 1993), the effect of diffusional fractionation on the $\Delta^{17}O$ of atmospheric CO_2 is

−0.168 ‰ regardless of the anomaly of the CO_2 entering the leaf, and the model results confirm this at low c_m/c_a ratios (Fig. 5c and d, inset).

At a high c_m/c_a ratio, $\Delta^{17}O_a$ is dominated by the back-diffusion flux of CO_2 that has equilibrated with water. As a consequence, $\Delta^{17}O_a$ converges to a common value that is independent of the anomaly of the CO_2 entering the cuvette and is determined by the isotopic composition of leaf water. Figure 5 confirms that the end-member is equal to the $\Delta^{17}O$ of CO_2 in equilibrium with leaf water, $\Delta^{17}O_m$. In fact, when $\Delta^{17}O_a$=$\Delta^{17}O_m$, $\Delta^{17}O_a$ does not change with c_m/c_a, indicating that in this case the $\Delta^{17}O$ of the CO_2 diffusing back from the leaf is the same as the $\Delta^{17}O(CO_2)$ entering the leaf.

$\overline{a}_{18}$ is the overall discrimination occurring during the diffusion of $^{12}C^{18}O^{16}O$ from the ambient air surrounding the leaf to the CO_2-H_2O exchange site (see Table 2 for the list of variables). In our study $\overline{a}_{18}$ ranges from 5 ‰ to 7.2 ‰, lower than the literature estimate of 7.4 ‰ (Farquhar et al., 1993). $\overline{a}_{18}$ depends on the ratio of stomatal conductance, which is associated with a strong fractionation of 8.8 ‰, to mesophyll conductance with an associated fractionation of only 0.8 ‰. Therefore, the higher the ratio (g_s/g_{m18}) the lower the $\overline{a}_{18}$ (Table S2). The difference in $\overline{a}_{18}$ of 2.4 ‰ between the literature value of 7.4 ‰ and the lowest $\overline{a}_{18}$ estimate in this study will introduce an error of only 0.046 ‰ in the $\Delta^{17}O$ value (see Eq. 6). The uncertainty $\overline{a}_{18}$ has lower influence on the $\Delta_A\Delta^{17}O$ of C_3 plants compared to C_4 plants since the diffusional fractionation is less important at the higher c_m/c_a ratio where C_3 plants operate.

5.3 Global average value of $\Delta_A\Delta^{17}O$ and $\Delta^{17}O$ isoflux

We can use the established relationship between $\Delta_A\Delta^{17}O$ and $\Delta^{17}O_a-\Delta^{17}O_{wes}$ for a certain c_m/c_a ratio to provide a bottom-up estimate for the global effect of photosynthesis on $\Delta^{17}O$ in atmospheric CO_2, based on data obtained in real gas exchange experiments. For this, we use results from a recent modeling study, which provides global average values for CO_2 and leaf water ($\Delta^{17}O(CO_2) = -0.168$ ‰, $\Delta^{17}O(H_2O_{-leaf}) = -0.067$ ‰; Koren et al., 2019; Figs. S13 and 14). The $\Delta^{17}O(CO_2)$ values agree well with the limited amount of available measurements (Table 3).

To extrapolate $\Delta_A\Delta^{17}O$ determined in the leaf-scale experiments to the global scale, global average c_m/c_a ratios of 0.7 and 0.3 are used for C_3 and C_4 plants, respectively, similar to previous studies (Hoag et al., 2005; Liang et al., 2017b). From the SIBCASA model results we obtained an annual variability of c_i/c_a values with a standard deviation of 0.12 and 0.17 for C_4 and C_3 plants, respectively (Fig. S15) (Schaefer et al., 2008; Koren et al., 2019). We use this variability as the upper limit of the error estimate for c_m/c_a, as shown in the light orange and light pink shaded areas in Fig. 4b. This error is converted to an error in $\Delta_A\Delta^{17}O$ using the relation with c_m/c_a. Based on the linear dependency of $\Delta_A\Delta^{17}O$ and $\Delta^{17}O_a-\Delta^{17}O_{wes}$, we estimate the $\Delta_A\Delta^{17}O$ for tropospheric CO_2 based on the $\Delta^{17}O$ of leaf water and c_m/c_a ratio. In Fig. 4b, the vertical dashed black line indicates $\Delta^{17}O_a-\Delta^{17}O_{wes}$ obtained from the 3D global model (Koren et al., 2019). The results of the global estimate and parameters used for the extrapolation of a leaf-scale study to the global scale are summarized in Table 3.

The $\delta^{17}O$ value of atmospheric CO_2 (21.53 ‰) is calculated from the global $\delta^{18}O$ and $\Delta^{17}O$ values (41.5 ‰ and −0.168 ‰, respectively) (Koren et al., 2019). The $\delta^{17}O$ and $\delta^{18}O$ values of global mean leaf water are calculated from the soil water. A global mean $\delta^{18}O$ value of soil water is −8.4 ‰ assuming soil water to be similar to precipitation (Bowen and Revenaugh, 2003; Koren et al., 2019). The $\delta^{17}O$ value of soil water is −4.4 ‰, calculated using Eq. (7) (Luz and Barkan, 2010).

$$\ln\left(\delta^{17}O_{soil}+1\right) = 0.528 \times \ln\left(\delta^{18}O_{soil}+1\right) + 0.033 \qquad (7)$$

$\delta^{17}O$ and $\delta^{18}O$ of leaf water are calculated from $\delta^{17}O$ and $\delta^{18}O$ of soil water with fractionation factors of 1.0043 and 1.0084, respectively (Hofmann et al., 2017; Koren et al., 2019). The fractionation factor for $\delta^{17}O$ is calculated using $\alpha^{17} = \left(\alpha^{18}\right)^{\text{trans}}$ with $\lambda_{trans} = 0.516$, assuming relative humidity to be 75 % (Landais et al., 2006). The $\delta^{17}O$ and $\delta^{18}O$ values of global mean leaf water are then −0.136 ‰ and −0.131 ‰, respectively. Thus, the difference between global atmospheric CO_2 and leaf water is $\delta^{17}O_{CO_2-water} = 21.666$ ‰ and $\delta^{18}O_{CO_2-water} = 41.631$ ‰. This yields $\Delta^{17}O_{CO_2-water} = -0.101$ ‰, and this value is indicated as a dashed black line in Fig. 4. The gray shaded area indicates the propagated error using the standard deviation of the relevant parameters in 180×360 grid boxes for 12 months of leaf water and 45 × 60 grid boxes for 24 months for CO_2 (Koren et al., 2019). In Fig. 4b, the intersection between the vertical dashed black line and the discrimination lines for the representative c_m/c_a ratios of C_3 and C_4 plants corresponds to the $\Delta_A\Delta^{17}O$ value of C_3 and C_4 plants. For C_4 plants ($c_m/c_a = 0.3$) this yields $\Delta_A\Delta^{17}O = -0.3$ ‰ (dashed gray line in Fig. 4b), and for C_3 plants it yields ($c_m/c_a = 0.7$) $\Delta_A\Delta^{17}O = -0.65$ ‰ (dashed black line in Fig. 4b).

Three main factors contribute to the uncertainty of the extrapolated $\Delta_A\Delta^{17}O$ value. The first is the measurement error, which contributes 0.25 ‰ (standard error for individual experiments). The second factor is the uncertainty in the difference between $\Delta^{17}O$ of atmospheric CO_2 and leaf water, and we use results from the global model to estimate an error. For $\Delta^{17}O$ of atmospheric CO_2, statistics for all 45 × 60 grid boxes for 24 months (2012–2013) show a range of −0.218 ‰ to −0.151 ‰, with a mean of −0.168 ‰ and a standard deviation of 0.013 ‰ (Fig. S13). For $\Delta^{17}O$ of the leaf water statistics for all 180 × 360 grid boxes for 12 months show a range of −0.236 ‰ and −0.027 ‰ (Fig. S14). The mean is −0.067 ‰ with a standard deviation of 0.041 ‰. From the combined errors we estimate the error in ($\Delta^{17}O_a-\Delta^{17}O_{wes}$) to be 0.043 ‰. The third uncertainty in the extrapolation of

Table 3. Summary of the parameters used for the extrapolation of leaf-scale experiments to the global scale and the results obtained, as well as an overview of available $\Delta^{17}O$ measurements.

Parameter	Value	ref
Parameters and values used for global estimation		
GPP	$120\,PgC\,yr^{-1}$	Beer et al. (2010)
f_{C4}	23 %	Still et al. (2003)
f_{C3}	77 %	Still et al. (2003)
c_m/c_a (C_3)	0.7	Hoag et al. (2005)
c_m/c_a (C_4)	0.3	Hoag et al. (2005)
$\Delta^{17}O$ leaf water (global mean, modeled)	-0.067 ± 0.04 ‰	Koren et al. (2019)
$\Delta^{17}O$ CO_2 (global mean, modeled)	-0.168 ± 0.013 ‰	Koren et al. (2019)
$\Delta_A\Delta^{17}O$ (global mean for C_4)	-0.3 ± 0.18 ‰	Fig. 5b, for c_m/c_a ratio of 0.3
$\Delta_A\Delta^{17}O$ (global mean for C_3)	-0.65 ± 0.18 ‰	Fig. 5b, for c_m/c_a ratio of 0.7
$\Delta_A\Delta^{17}O$ (global mean for whole vegetation)	-0.57 ± 0.14 ‰	Eq. (13)
$\Delta_A\Delta^{17}O$-isoflux (global mean for C_4)	-7.3 ± 4 ‰ $PgC\,yr^{-1}$	Eq. (14), only for C_4
$\Delta_A\Delta^{17}O$-isoflux (global mean for C_3)	-53 ± 15 ‰ $PgC\,yr^{-1}$	Eq. (14), only for C_3
$\Delta_A\Delta^{17}O$-isoflux (global mean for whole vegetation)	-60 ± 15 ‰ $PgC\,yr^{-1}$	Eq. (14)
$\Delta_A\Delta^{17}O$-isoflux (global mean for whole vegetation)	-47 ‰ $PgC\,yr^{-1}$	Hoag et al. (2005)
$\Delta_A\Delta^{17}O$-isoflux (global mean for whole vegetation)	-42 ‰ $PgC\,yr^{-1}$ to -92 ‰ $PgC\,yr^{-1}$	Hofmann et al. (2017)
$\Delta^{17}O$ value of tropospheric CO_2		
$\Delta^{17}O(CO_2)$ for CO_2 samples collected at La Jolla, UCSD (California, USA) (1990–2000)	-0.173 ± 0.046 ‰	Thiemens et al. (2014)
$\Delta^{17}O(CO_2)$ for CO_2 samples collected in Israel	0.034 ± 0.010 ‰	Barkan and Luz (2012)
$\Delta^{17}O(CO_2)$ for CO_2 samples collected in the South China Sea (2013–2014)	-0.159 ± 0.084 ‰	Liang et al. (2017b, a)
$\Delta^{17}O(CO_2)$ for CO_2 samples collected in Taiwan (2012–2015)	-0.150 ± 0.080 ‰	Liang et al. (2017b, a)
$\Delta^{17}O(CO_2)$ for CO_2 samples collected in California (USA) (2015)	-0.177 ± 0.029 ‰	Liang et al. (2017b, a)
$\Delta^{17}O(CO_2)$ for CO_2 samples collected in Göttingen (Germany) (2010–2012)	-0.122 ± 0.065 ‰	Hofmann et al. (2017)

$\Delta^{17}O$ comes from the uncertainty in the c_m/c_a ratio. For C_3 and C_4 plants, these errors are indicated by the light orange and light blue shadings in Fig. 4b.

Taking these uncertainties into account leads to a mean value of $\Delta_A\Delta^{17}O = -0.3 \pm 0.18$ ‰ for C_4 plants and $\Delta_A\Delta^{17}O = -0.65 \pm 0.18$ ‰ for C_3 plants. The leaf-scale discrimination against $\Delta^{17}O$ is then extrapolated to global vegetation using these representative values of $\Delta_A\Delta^{17}O$ and the relative fractions of photosynthesis by C_4 and C_3 plants, respectively, as follows:

$$\Delta_A^{17}O_{global} = f_{C_4} \times \Delta_A^{17}O_{C_4} + f_{C_3} \times \Delta_A^{17}O_{C_3}, \tag{8}$$

where f_{C_4} and f_{C_3} are the photosynthesis-weighted global coverage of C_4 and C_3 vegetation. $\Delta_A\Delta^{17}O_{C_4}$ and $\Delta_A\Delta^{17}O_{C_3}$ quantify the discrimination against $\Delta^{17}O$ by C_4 and C_3 plants, which are calculated using estimated values of c_m/c_a from a model. Using assimilation-weighted fractions of 23 % for C_4 and 77 % for C_3 vegetation (Still et al., 2003), the global mean value of $\Delta_A\Delta^{17}O$ obtained from Eq. (8) is -0.57 ± 0.14 ‰.

Isoflux is the product of isotope composition and gross mass flux of the molecule. In the case of assimilation, the net flux $F_A = F_{AL} - F_{LA}$ is multiplied with the discrimination associated with assimilation (Ciais et al., 1997a). F_{LA} and F_{AL} are total CO_2 fluxes from leaf to the atmosphere and from atmosphere to leaf, respectively. The global-scale $\Delta^{17}O_A$ isoflux is calculated by multiplying the discrimination with the assimilation flux as follows:

$$F_A \times \Delta_A^{17}O = A \times \left(f_{C_4} \times \Delta_A^{17}O_{C_4} + f_{C_3} \times \Delta_A^{17}O_{C_3}\right), \tag{9}$$

where $A = 0.88 \times GPP$ is the terrestrial assimilation rate. The factor 0.88 accounts for the fraction of CO_2 released due to autotrophic respiration (Ciais et al., 1997a). The $\Delta_A\Delta^{17}O$ isoflux due to photosynthesis is calculated using a GPP value of $120\,PgC\,yr^{-1}$ (Beer et al., 2010) and $A = 0.88 \times GPP$, resulting in an isoflux of $-60 \pm 15\,‰\,PgC\,yr^{-1}$ globally. This is the first global estimate of $\Delta_A\Delta^{17}O$ based on direct measurements of the discrimination during assimilation. Our value is in good agreement with previous model estimates. Hofmann et al. (2017) estimated an isoflux ranging from $-42\,‰\,PgC\,yr^{-1}$ to $-92\,‰\,PgC\,yr^{-1}$ (converted to a reference line with $\lambda = 0.528$) using an average c_m/c_a ratio of 0.7 for both C_4 and C_3 plants and $\Delta^{17}O$ of $-0.147\,‰$ for atmospheric CO_2. A model-estimated value from Hoag et al. (2005) is $-47\,‰\,PgC\,yr^{-1}$ (converted to our reference slope of $\lambda = 0.528$), derived with a more simple model and using $\Delta^{17}O$ of $-0.146\,‰$ with c_m/c_a ratio of 0.33 and 0.66 for C_4 and C_3 plants, respectively.

The main uncertainty in the extrapolation of $\Delta_A\Delta^{17}O$ from the leaf experiments to the global scale is the uncertainty in the c_m/c_a ratio. The error from the uncertainty in c_m/c_a ratio increases when the relative difference in $\Delta^{17}O$ between CO_2 and leaf water increases (Fig. 5b). It is difficult to determine a single representative c_m value for different plants because this value would need to be properly weighted with temperature, irradiance, CO_2 mole fraction, and other environmental factors (Flexas et al., 2008, 2012; Shrestha et al., 2019). Recent developments in laser spectroscopy techniques (McManus et al., 2005; Nelson et al., 2008; Tuzson et al., 2008; Kammer et al., 2011) might enable more and easier measurements of c_m/c_a both in the laboratory and under field conditions. This could lead to a better understanding of variations in the c_m/c_a ratio among plant species temporally, spatially, and environmentally.

6 Conclusions

In order to directly quantify the effect of photosynthetic gas exchange on the $\Delta^{17}O$ of atmospheric CO_2, gas exchange experiments were carried out in leaf cuvettes using two C_3 plants (sunflower and ivy) and one C_4 plant (maize) with isotopically normal and slightly anomalous (^{17}O-enriched) CO_2. Results for ^{18}O agree with results reported in the literature previously. Our results for $\Delta^{17}O$ confirm that the formalism developed by Farquhar and others for $\delta^{18}O$ is also applicable to the evaluation of $\Delta^{17}O$. In particular, our experiments confirm that two parameters determine the effect of photosynthesis on CO_2: (1) the $\Delta^{17}O$ difference between the incoming CO_2 and CO_2 in equilibrium with leaf water and (2) the c_m/c_a ratio, which determines the degree of backflux of isotopically exchanged CO_2 from the mesophyll to the atmosphere. At low c_m/c_a ratios, $\Delta_A\Delta^{17}O$ is mainly influenced by the diffusional fractionation. Under our experimental conditions, the isotopic effect increased with c_m/c_a, e.g., $\Delta_A\Delta^{17}O$ was $-0.3\,‰$ and $-0.65\,‰$ for maize and sunflower with c_m/c_a ratios of 0.3 and 0.7, respectively. However, experiments with mass independently fractionated CO_2 demonstrate that the results depend strongly on the $\Delta^{17}O$ difference between the incoming CO_2 and CO_2 in equilibrium with leaf water. This is supported by calculations with a leaf cuvette model.

$\delta^{18}O$ is largely affected by kinetic and equilibrium processes between CO_2 and leaf water, and also leaf water isotopic inhomogeneity and dynamics. The $\Delta^{17}O$ variation is much smaller compared to $\delta^{18}O$ and is better defined since conventional biogeochemical processes that modify $\delta^{17}O$ and $\delta^{18}O$ follow a well-defined three-isotope fractionation slope. Results from the leaf exchange experiments were upscaled to the global atmosphere using modeled values for $\Delta^{17}O$ of leaf water and CO_2, which results in $\Delta_A\Delta^{17}O = -0.57 \pm 0.14\,‰$ and a value for the $\Delta^{17}O$ isoflux of $-60 \pm 15\,‰\,PgC\,yr^{-1}$. This is the first study that provides such an estimate based on direct leaf chamber measurements, and the results agree with previous $\Delta^{17}O$ calculations. The largest contribution to the uncertainty originates from uncertainty in the c_m/c_a ratio and the largest contributions to the isoflux come from C_3 plants, which have both a higher share of the total assimilation and higher discrimination. $\Delta_A\Delta^{17}O$ is less sensitive to c_m/c_a ratios at lower values of c_m/c_a, for instance for C_4 plants such as maize.

$\Delta^{17}O$ of tropospheric CO_2 is controlled by photosynthetic gas exchange, respiration, soil invasion, and stratospheric influx. The stratospheric flux is well established and the effect of photosynthetic gas exchange can now be quantified more precisely. To untangle the contribution of each component to the $\Delta^{17}O$ atmospheric CO_2, we recommend measuring the effects of foliage respiration and soil invasion both in the laboratory and at the ecosystem scale.

Code and data availability. The data used in this study are included in the paper either with figures or tables. The python code for the cuvette model is available at https://git.wur.nl/leaf_model (last access: 23 March 2020, Koren et al., 2020).

Supplement. The supplement related to this article is available online at: https://doi.org/10.5194/bg-17-3903-2020-supplement.

Author contributions. GAA and TR designed the main idea of the study. GAA and TP designed the leaf cuvette setup. TP monitors plant growth. GAA and TR designed the CO_2 extraction and CO_2-O_2 exchange system. GAA conducted all the measurements. GK provided the leaf cuvette model. WP enabled the work within the ASICA project. All authors discussed the results at different steps of the project. GAA and TR prepared the manuscript with contributions from all the co-authors.

Competing interests. The authors declare that they have no conflict of interest.

Acknowledgements. The authors thank Leonard I. Wassenaar and Stefan Terzer-Wassmuth from the International Atomic and Energy Agency, Vienna, for supplying water standards. The authors thank Eugeni Barkan and Rolf Vieten from the Hebrew University of Jerusalem for calibration of our O_2 and CO_2 working gases. We are grateful to Amaelle Landais from Laboratoire des Sciences Du Climat et de l'Environnement Université Paris-Saclay for measuring the $\Delta^{17}O$ of leaf water samples for our study. The authors thank Amzad Laskar for the useful discussion during the design of the experiment. This work is funded by the EU ERC project ASICA.

Financial support. This research has been supported by the European Research Council (ASICA (grant no. 649087)).

Review statement. This paper was edited by Aninda Mazumdar and reviewed by two anonymous referees.

References

Adnew, G. A., Hofmann, M. E. G., Paul, D., Laskar, A., Surma, J., Albrecht, N., Pack, A., Schwieters, J., Koren, G., Peters, W., and Röckmann, T.: Determination of the triple oxygen and carbon isotopic composition of CO_2 from atomic ion fragments formed in the ion source of the 253 Ultra High-Resolution Isotope Ratio Mass Spectrometer, Rapid Commun. Mass. Sp., 33, 17 pp., 2019.

Badger, M. R. and Price, G. D.: The role of carbonic anhydrase in photosynthesis, Annu. Rev. Plant Biol., 45, 23 pp., 1994.

Bao, H., Cao, X., and Hayles, J. A.: Triple oxygen isotopes: fundamental relationships and applications, Annu. Rev. Earth Planet. Sci., 44, 29 pp., 2016.

Barbour, M. M., Evans, J. R., Simonin, K. A., and von Caemmerer, S.: Online CO_2 and H_2O oxygen isotope fractionation allows estimation of mesophyll conductance in C_4 plants, and reveals that mesophyll conductance decreases as leaves age in both C_4 and C_3 plants, New Phytol., 210, 875–889, https://doi.org/10.1111/nph.13830, 2016.

Barkan, E. and Luz, B.: High precision measurements of $^{17}O/^{16}O$ and $^{18}O/^{16}O$ ratios in H_2O, Rapid Commun. Mass. Sp., 19, 3737–3742, https://doi.org/10.1002/rcm.2250, 2005.

Barkan, E. and Luz, B.: Diffusivity fractionations of $H_2^{16}O/H_2^{17}O$ and $H_2^{16}O/H_2^{18}O$ in air and their implications for isotope hydrology, Rapid Commun. Mass. Sp., 21, 6 pp., 2007.

Barkan, E. and Luz, B.: The relationships among the three stable isotopes of oxygen in air, seawater and marine photosynthesis, Rapid Commun. Mass. Sp., 25, 2 pp., 2011.

Barkan, E. and Luz, B.: High-precision measurements of $^{17}O/^{16}O$ and $^{18}O/^{16}O$ ratios in CO_2, Rapid Commun. Mass. Sp., 26, 2733–2738, https://doi.org/10.1002/rcm.6400, 2012.

Barkan, E., Musan, I., and Luz, B.: High-precision measurements of $\delta^{17}O$ and ^{17}O-excess of NBS19 and NBS18, Rapid Commun. Mass. Sp., 29, 2219–2224, https://doi.org/10.1002/rcm.7378, 2015.

Beer, C., Reichstein, M., Tomelleri, E., Ciais, P., Jung, M., Carvalhais, N., Rodenbeck, C., Arain, M. A., Baldocchi, D., Bonan, G. B., Bondeau, A., Cescatti, A., Lasslop, G., Lindroth, A., Lomas, M., Luyssaert, S., Margolis, H., Oleson, K. W., Roupsard, O., Veenendaal, E., Viovy, N., Williams, C., Woodward, F. I., and Papale, D.: Terrestrial gross carbon dioxide uptake: global distribution and covariation with climate, Science, 329, 834–838, https://doi.org/10.1126/science.1184984, 2010.

Boering, K. A.: Observations of the anomalous oxygen isotopic composition of carbon dioxide in the lower stratosphere and the flux of the anomaly to the troposphere, Geophys. Res. Lett., 31, L03109, https://doi.org/10.1029/2003GL018451, 2004.

Booth, B. B. B., Jones, C. D., Collins, M., Totterdell, I. J., Cox, P. M., Sitch, S., Huntingford, C., Betts, R. A., Harris, G. R., and Lloyd, J.: High sensitivity of future global warming to land carbon cycle processes, Environ. Res. Lett., 7, 024002, https://doi.org/10.1088/1748-9326/7/2/024002, 2012.

Bowen, G. J. and Revenaugh, J.: Interpolating the isotopic composition of modern meteoric precipitation, Water Resour. Res., 39, 1299, https://doi.org/10.1029/2003WR002086, 2003.

Brand, W. A., Assonov, S. S., and Coplen, T. B.: Correction for the ^{17}O interference in $\delta^{13}C$ measurements when analyzing CO_2 with stable isotope mass spectrometry (IUPAC Technical Report), Pure Appl. Chem., 82, 1719–1733, https://doi.org/10.1351/pac-rep-09-01-05, 2010.

Cao, X. and Liu, Y.: Equilibrium mass-dependent fractionation relationships for triple oxygen isotopes, Geochim. Cosmochim. Ac., 75, 7435–7445, https://doi.org/10.1016/j.gca.2011.09.048, 2011.

Cernusak, L. A., Barbour, M. M., Arndt, S. K., Cheesman, A. K., English, N. B., Feild, T. S., Helliker, B. R., Holloway-Phillips, M. M., Holtum, J. A., Kahmen, A., McInerney, F. A., Munksgaard, N. C., Simonin, K. A., Song, X., Stuart-Williams, H., West, J. B., and Farquhar, G. D.: Stable isotopes in leaf water of terrestrial plants, Plant Cell Environ., 39, 1087–1102, https://doi.org/10.1111/pce.12703, 2016.

Ciais, P., Denning, A. S., Tans, P. P., Berry, J. A., Randall, D. A., Collatz, G. J., Sellers, P. J., White, J. W. C., Trolier, M., Meijer, H. A. J., Francey, R. J., Monfray, P., and Heimann, M.: A three-dimensional synthesis study of $\delta^{18}O$ in atmospheric CO_2: 1. Surface fluxes, J. Geophys. Res., 102, 5857–5872, https://doi.org/10.1029/96jd02360, 1997a.

Ciais, P., Tans, P. P., Denning, A. S., Francey, R. J., Trolier, M., Meijer, H. A. J., White, J. W. C., Berry, J. A., Randall, D. A., and Collatz, G. J.: A three-dimensional synthesis study of $\delta^{18}O$ in atmospheric CO_2: 2. Simulations with the TM2 transport model, J. Geophys. Res., 102, 5873–5883, https://doi.org/10.1029/96JD02361, 1997b.

Cuntz, M.: A dent in carbon's gold standard, Nature, 477, 547–548, 2011.

Cuntz, M., Ciais, P., Hoffmann, G., Allison, C. E., Francey, R. J., Knorr, W., Tans, P. P., White, J. W. C., and Levin, I.: A comprehensive global three-dimensional model of $\delta^{18}O$ in atmospheric CO_2: 2. Mapping the atmospheric signal J. Geophys. Res., 108, 4528, https://doi.org/10.1029/2002JD003154, 2003a.

Cuntz, M., Ciais, P., Hoffmann, G., and Knorr, W.: A comprehensive global three-dimensional model of $\delta^{18}O$ in atmospheric

CO_2: 1. Validation of surface processes, J. Geophys. Res.-Atmos., 108, 24 pp., 2003b.

DiMario, R. J., Quebedeaux, J. C., Longstreth, D. J., Dassanayake, M., Hartman, M. M., and Moroney, J. V.: The cytoplasmic carbonic anhydrases βCA_2 and βCA_4 are required for optimal plant growth at low CO_2, Plant Physiol., 171, 13 pp., 2016.

Evans, J. R., Sharkey, T. D., Berry, J. A., and Farquhar, G. D.: Carbon isotope discrimination measured concurrently with gas exchange to investigate CO_2 diffusion in leaves of higher plants, Funct. Plant. Biol., 13, 11 pp., 1986.

Fabre, N., Reiter, I. M., Becuwe-Linka, N., Genty, B., and Rumeau, D.: Characterization and expression analysis of genes encoding alpha and beta carbonic anhydrases in Arabidopsis, Plant Cell Environ., 30, 617–629, https://doi.org/10.1111/j.1365-3040.2007.01651.x, 2007.

Farquhar, G. D. and Gan, K. S.: On the progressive enrichment of the oxygen isotopic composition of water along a leaf, Plant Cell Environ., 26, 18 pp., 2003.

Farquhar, G. D. and Lloyd, J.: Carbon and oxygen isotope effects in the exchange of carbon dioxide between terrestrial plants and the atmosphere, Stable isotopes and plant carbon-water relations, Acadamic Press Inc., London, 47 pp., 1993.

Farquhar, G. D. and Richards, R. A.: Isotopic composition of plant carbon correlates with water-use efficiency of wheat genotypes, Funct. Plant Biol., 11, 11 pp., 1984.

Farquhar, G. D., Ehleringer, J. R., and Hubic, K. T.: Carbon isotope discrimination and photosynthesis, Annu. Rev. Plant Phys., 40, 34 pp., 1989.

Farquhar, G. D., Lloyd, J., Taylor, J. A., Flanagan, L. B., Syvertsen, J. P., Hubick, K. T., Wong, S. C., and Ehleringer, J. R.: Vegetation effects on the isotope composition of oxygen in atmospheric CO_2, Nature, 363, 4 pp., 1993.

Flanagan, L. B. and Ehleringer, J. R.: Ecosystem-atmosphere CO_2 exchange: interpreting signals of change using stable isotope ratios, Trends Ecol. Evol., 13, 4 pp., 1998.

Flexas, J., Ribas-Carbo, M., Diaz-Espejo, A., Galmes, J., and Medrano, H.: Mesophyll conductance to CO_2: current knowledge and future prospects, Plant Cell Environ., 31, 19 pp., 2008.

Flexas, J., Barbour, M. M., Brendel, O., Cabrera, H. M., Carriquí, M., Díaz-Espejo, A., Douthe, C., Dreyer, E., Ferrio, J. P., and Gago, J.: Mesophyll diffusion conductance to CO_2: an unappreciated central player in photosynthesis, Plant Sci., 193, 14 pp., 2012.

Francey, R. J. and Tans, P. P.: Latitudinal variation in oxygen-18 of atmospheric CO_2, Nature, 327, 2 pp., 1987.

Fredeen, A. L., Gamon, J. A., and Field, C. B.: Responses of photosynthesis and carbohydrate-partitioning to limitations in nitrogen and water availability in field-grown sunflower, Plant Cell Environ., 14, 7 pp., 1991.

Friedli, H., Siegenthaler, U., Rauber, D., and Oeschger, H.: Measurements of concentration, $^{13}C/^{12}C$ and $^{18}O/^{16}O$ ratios of tropospheric carbon dioxide over Switzerland, Tellus B, 39, 8 pp., 1987.

Gan, K. S., Wong, S. C., Yong, J. W. H., and Farquhar, G. D.: ^{18}O spatial patterns of vein xylem water, leaf water, and dry matter in cotton leaves, Plant Physiol., 130, 13 pp., 2002.

Gan, K. S., Wong, S. C., Yong, J. W. H., and Farquhar, G. D.: Evaluation of models of leaf water ^{18}O enrichment using measurements of spatial patterns of vein xylem water, leaf water and dry matter in maize leaves, Plant Cell Environ., 26, 16 pp., 2003.

Gillon, J. and Yakir, D.: Influence of carbonic anhydrase activity in terrestrial vegetation on the ^{18}O content of atmospheric CO_2, Science, 291, 3 pp., 2001.

Gillon, J. S. and Yakir, D.: Internal conductance to CO_2 diffusion and $C^{18}OO$ discrimination in C_3 leaves, Plant Physiol., 123, 13 pp., 2000a.

Gillon, J. S. and Yakir, D.: Naturally low carbonic anhydrase activity in C_4 and C_3 plants limits discrimination against $C^{18}OO$ during photosynthesis, Plant Cell Environ., 23, 12 pp., 2000b.

Heidenreich, J. E. and Thiemens, M. H.: A non-mass-dependent isotope effect in the production of ozone from molecular oxygen J. Chem. Phys., 78, 3 pp., 1983.

Heidenreich, J. E. and Thiemens, M. H.: A non-mass-dependent oxygen isotope effect in the production of ozone from molecular oxygen: The role of molecular symmetry in isotope chemistry J. Chem. Phys., 84, 5 pp., 1986.

Hoag, K. J., Still, C. J., Fung, I. Y., and Boering, K. A.: Triple oxygen isotope composition of tropospheric carbon dioxide as a tracer of terrestrial gross carbon fluxes, Geophys. Res. Lett., 32, L02802, https://doi.org/10.1029/2004gl021011, 2005.

Hofmann, M. E. G., Horváth, B., Schneider, L., Peters, W., Schützenmeister, K., and Pack, A.: Atmospheric measurements of $\Delta^{17}O$ in CO_2 in Göttingen, Germany reveal a seasonal cycle driven by biospheric uptake, Geochim. Cosmochim. Ac., 199, 143–163, https://doi.org/10.1016/j.gca.2016.11.019, 2017.

Johnson, K. S.: Carbon dioxide hydration and dehydration kinetics in seawater 1, Limnol. Oceanogr., 27, 6 pp., 1982.

Jung, M., Schwalm, C., Migliavacca, M., Walther, S., Camps-Valls, G., Koirala, S., Anthoni, P., Besnard, S., Bodesheim, P., Carvalhais, N., Chevallier, F., Gans, F., Goll, D. S., Haverd, V., Köhler, P., Ichii, K., Jain, A. K., Liu, J., Lombardozzi, D., Nabel, J. E. M. S., Nelson, J. A., O'Sullivan, M., Pallandt, M., Papale, D., Peters, W., Pongratz, J., Rödenbeck, C., Sitch, S., Tramontana, G., Walker, A., Weber, U., and Reichstein, M.: Scaling carbon fluxes from eddy covariance sites to globe: synthesis and evaluation of the FLUXCOM approach, Biogeosciences, 17, 1343–1365, https://doi.org/10.5194/bg-17-1343-2020, 2020.

Kaiser, J., Röckmann, T., and Brenninkmeijer, C. A. M.: Contribution of mass-dependent fractionation to the oxygen isotope anomaly of atmospheric nitrous oxide, J. Geophys. Res., 109, D03305, https://doi.org/10.1029/2003JD004088, 2004.

Kammer, A., Tuzson, B., Emmenegger, L., Knohl, A., Mohn, J., and Hagedorn, F.: Application of a quantum cascade laser-based spectrometer in a closed chamber system for real-time $\delta^{13}C$ and $\delta^{18}O$ measurements of soil-respired CO_2, Agr. Forest Meteorol., 151, 9 pp., 2011.

Kawagucci, S., Tsunogai, U., Kudo, S., Nakagawa, F., Honda, H., Aoki, S., Nakazawa, T., Tsutsumi, M., and Gamo, T.: Long-term observation of mass-independent oxygen isotope anomaly in stratospheric CO_2, Atmos. Chem. Phys., 8, 6189–6197, https://doi.org/10.5194/acp-8-6189-2008, 2008.

Koren, G., Adnew, G. A., Röckmann, T., and Peters, W.: Leaf conductance model for $\Delta^{17}O$ in CO_2, Git@WUR, available at: https://git.wur.nl/leaf_model, last access: 23 March 2020.

Koren, G., Schneider, L., van der Velde, I. R., van Schaik, E., Gromov, S. S., Adnew, G. A., Mrozek Martino, D. J., Hofmann, M. E. D., Liang, M.-C., Mahata, S., Bergamaschi, P., van der Laan-

Luijkx, I. T., Krol, M. C., Röckmann, T., and Peters, W.: Global 3-D Simulations of the Triple Oxygen Isotope Signature $\Delta^{17}O$ in Atmospheric CO_2, J. Geophys. Res.-Atmos., 124, 28 pp., 2019.

Lämmerzahl, P., Röckmann, T., and Brenninkmeijer, C. A. M.: Oxygen isotope composition of stratospheric carbon dioxide, Geophys. Res. Lett., 29, 23-1–23-4, https://doi.org/10.1029/2001gl014343, 2002.

Landais, A., Barkan, E., Yakir, D., and Luz, B.: The triple isotopic composition of oxygen in leaf water, Geochim. Cosmochim. Ac., 70, 4105–4115, 10.1016/j.gca.2006.06.1545, 2006.

Landais, A., Barkan, E., and Luz, B.: Record of $\delta^{18}O$ and ^{17}O-excess in ice from Vostok Antarctica during the last 150,000 years, Geophys. Res. Lett., 35, L02709, https://doi.org/10.1029/2007gl032096, 2008.

Laskar, A. H., Mahata, S., and Liang, M.-C.: Identification of anthropogenic CO_2 using triple oxygen and clumped isotopes, Environ. Sci. Technol., 50, 18 pp., https://doi.org/10.1021/acs.est.6b02989, 2016.

Liang, M.-C. and Mahata, S.: Oxygen anomaly in near surface carbon dioxide reveals deep stratospheric intrusion, Scientific Reports, 5, 11352, https://doi.org/10.1038/srep11352, 2015.

Liang, M.-C., Blake, G. A., Lewis, B. R., and Yung, Y. L.: Oxygen isotopic composition of carbon dioxide in the middle atmosphere, P. Natl. Acad. Sci. USA, 104, 4 pp., 2006.

Liang, M.-C., Mahata, S., Laskar, A. H., and Bhattacharya, S. K.: Spatiotemporal variability of oxygen isotope anomaly in near surface air CO_2 over urban, semi-urban and ocean areas in and around Taiwan, Aerosol Air Qual. Res., 17, 24 pp., 2017a.

Liang, M.-C., Mahata, S., Laskar, A. H., Thiemens, M. H., and Newman, S.: Oxygen isotope anomaly in tropospheric CO_2 and implications for CO_2 residence time in the atmosphere and gross primary productivity, Scientific Reports, 7, 13180, https://doi.org/10.1038/s41598-017-12774-w, 2017b.

Luz, B. and Barkan, E.: Variations of $^{17}O/^{16}O$ and $^{18}O/^{16}O$ in meteoric waters, Geochim. Cosmochim. Ac., 74, 10 pp., 2010.

Lyons, J. R.: Transfer of mass-independent fractionation in ozone to other oxygen-containing radicals in the atmosphere, Geophys. Res. Lett., 28, 3231–3234, https://doi.org/10.1029/2000gl012791, 2001.

Mahata, S., Bhattacharya, S. K., Wang, C. H., and Liang, M.-C.: Oxygen isotope exchange between O_2 and CO_2 over hot platinum: an innovative technique for measuring $\Delta^{17}O$ in CO_2, Anal. Chem., 85, 6894–6901, 10.1021/ac4011777, 2013.

Matsuhisa, Y., Goldsmitrh, J. R., and Clayton, R. N.: Mechanisms of hydrothermal crystallization of quartz at 250 °C and 15 kbar, Geochim. Cosmochim. Ac., 42, 9 pp., 1978.

McManus, J. B., Nelson, D. D., Shorter, J. H., Jimenez, R., Herndon, S., Saleska, S., and Zahniser, M.: A high precision pulsed quantum cascade laser spectrometer for measurements of stable isotopes of carbon dioxide, J. Mod. Optic., 52, 12 pp., 2005.

Meijer, H. and Li, W.: The use of electrolysis for accurate ^{17}O and ^{18}O isotope measurements in water isotopes, Isot. Environ. Health S., 34, 20 pp., 1998.

Miller, J. B., Yakir, D., White, J. W. C., and Tans, P. P.: Measurement of $^{18}O/^{16}O$ in the soil-atmosphere CO_2 flux, Global Biogeochem. Cy., 13, 13 pp., 1999.

Miller, M. F.: Isotopic fractionation and the quantification of ^{17}O anomalies in the oxygen three-isotope system: an appraisal and geochemical significance, Geochim. Cosmochim. Ac., 66, 8 pp., 2002.

Miller, R. F., Berkshire, D. C., Kelley, J. J., and Hood, D. W.: Method for determination of reaction rates of carbon dioxide with water and hydroxyl ion in seawater, Environ. Sci. Technol., 5, 6 pp., 1971.

Mills, G. A. and Urey, H. C.: The kinetics of isotopic exchange between carbon dioxide, bicarbonate ion, carbonate ion and water, J. Am. Chem. Soc., 62, 7 pp., 1940.

Nelson, D. D., McManus, J. B., Herndon, S., Zahniser, M. S., Tuzson, B., and Emmenegger, L.: New method for isotopic ratio measurements of atmospheric carbon dioxide using a 4.3 µm pulsed quantum cascade laser, Appl. Phys. B-Lasers O., 90, 8 pp., 2008.

Osborn, H. L., Alonso-Cantabrana, H., Sharwood, R. E., Covshoff, S., Evans, J. R., Furbank, R. T., and von Caemmerer, S.: Effects of reduced carbonic anhydrase activity on CO_2 assimilation rates in Setaria viridis: a transgenic analysis, J. Exp. Bot., 68, 11 pp., 2017.

Pack, A. and Herwartz, D.: The triple oxygen isotope composition of the Earth mantle and understanding $\Delta^{17}O$ variations in terrestrial rocks and minerals, Earth. Planet. Sc. Lett., 390, 7 pp., 2014.

Peylin, P., Ciais, P., Denning, A. S., Tans, P. P., Berry, J. A., and White, J. W.: A 3-dimensional study of $\delta^{18}O$ in atmospheric CO_2: contribution of different land ecosystems, Tellus B, 51, 25 pp., 1999.

Pons, T. L. and Welschen, R. A. M.: Overestimation of respiration rates in commercially available clamp-on leaf chambers. Complications with measurement of net photosynthesis, Plant Cell Environ., 25, 5 pp., 2002.

Pons, T. L., Flexas, J., von Caemmerer, S., Evans, J. R., Genty, B., Ribas-Carbo, M., and Brugnoli, E.: Estimating mesophyll conductance to CO_2: methodology, potential errors, and recommendations J. Exp. Bot., 60, 7 pp., 2009.

Schaefer, K., Collatz, G. J., Tans, P., Denning, A. S., Baker, I., Berry, J., Prihodko, L., Suits, N., and Philpott, A.: Combined simple biosphere/Carnegie-Ames-Stanford approach terrestrial carbon cycle model, J. Geophys. Res., 113, G03034, https://doi.org/10.1029/2007JG000603, 2008.

Shaheen, R., Janssen, C., and Röckmann, T.: Investigations of the photochemical isotope equilibrium between O_2, CO_2 and O_3, Atmos. Chem. Phys., 7, 495–509, https://doi.org/10.5194/acp-7-495-2007, 2007.

Sharp, Z. D., Wostbrock, J. A. G., and Pack, A.: Mass-dependent triple oxygen isotope variations in terrestrial materials, Geochemical Perspectives Letters, 7, 27–31, https://doi.org/10.7185/geochemlet.1815, 2018.

Shrestha, A., Song, X., and Barbour, M. M.: The temperature response of mesophyll conductance, and its component conductances, varies between species and genotypes, Photosynth. Res., 141, 65–82, 2019.

Silverman, D. N.: Carbonic anhydrase: Oxygen-18 exchange catalyzed by an enzyme with rate-contributing Proton-transfer steps, Method. Enzymol., 87, 732–752, 1982.

Sitch, S., Friedlingstein, P., Gruber, N., Jones, S. D., Murray-Tortarolo, G., Ahlström, A., Doney, S. C., Graven, H., Heinze, C., Huntingford, C., Levis, S., Levy, P. E., Lomas, M., Poulter, B., Viovy, N., Zaehle, S., Zeng, N., Arneth, A., Bonan, G., Bopp, L., Canadell, J. G., Chevallier, F., Ciais, P., Ellis, R., Gloor, M., Peylin, P., Piao, S. L., Le Quéré, C., Smith, B., Zhu, Z., and Myneni, R.: Recent trends and drivers of regional sources and sinks of carbon dioxide, Biogeosciences, 12, 653–679, https://doi.org/10.5194/bg-12-653-2015, 2015.

Still, C. J., Berry, J. A., Collatz, G. J., and DeFries, R. S.: Global distribution of C_3 and C_4 vegetation: Carbon cycle implications, Global Biogeochem. Cy., 17, 1006, https://doi.org/10.1029/2001gb001807, 2003.

Thiemens, M. H.: Mass-independent isotope effects in planetary atmospheres and the early solar system, Science, 283, 4 pp., 1999.

Thiemens, M. H.: History and Applications of Mass-Independent Isotope Effects, Annu. Rev. Earth Pl. Sc., 34, 62 pp., https://doi.org/10.1146/annurev.earth.34.031405.125026, 2006.

Thiemens, M. H. and Heidenreich III, J. E.: Mass-independent fractionation of oxygen: a novel isotope effect and its possible cosmochemical implications, Science, 219, 1073–1075, https://doi.org/10.1126/science.219.4588.1073, 1983.

Thiemens, M. H., Jackson, T., Mauersberger, K., Schüler, B., and Morton, J.: Oxygen isotope fractionation in stratospheric CO_2, Geophys. Res. Lett., 18, 669–672, 1991.

Thiemens, M. H., Jackson, T., Zipf, E. C., Erdman, P. W., and van Egmond, C.: Carbon dioxide and oxygen isotope anomalies in the mesosphere and stratosphere, Science, 270, 3 pp., 1995.

Thiemens, M. H., Chakraborty, S., and Jackson, T. L.: Decadal $\Delta^{17}O$ record of tropospheric CO_2: Verification of a stratospheric componentin the troposphere, J. Geophys. Res.-Atmos., 119, 8 pp., https://doi.org/10.1002/2013JD020317, 2013.

Thiemens, M. K., Chakraborty, S., and Jackson, T. L.: Decadal $\Delta^{17}O$ record of tropospheric CO_2: Verification of a stratospheric component in the troposphere, J. Geophys. Res.-Atmos., 119, 8 pp., 2014.

Tuzson, B., Mohn, J., Zeeman, M. J., Werner, R. A., Eugster, W., Zahniser, M. S., Nelson, D. D., McManus, J. B., and Emmenegger, L.: High precision and continuous field measurements of $\delta^{13}C$ and $\delta^{18}O$ in carbon dioxide with a cryogen-free QCLAS, Appl. Phys. B-Lasers O., 92, 7 pp., 2008.

Uemura, R., Barkan, E., Abe, O., and Luz, B.: Triple isotope composition of oxygen in atmospheric water vapor, Geophys. Res. Lett., 37, L04402, https://doi.org/10.1029/2009GL041960, 2010.

van der Weijde, T., Kamei, C. L. A., Torres, A. F., Vermerris, W., Dolstra, O., Visser, R. G. F., and Trindade, L. M.: The potential of C_4 grasses for cellulosic biofuel production, Front. Plant. Sci., 4, 107, https://doi.org/10.3389/fpls.2013.00107, 2013.

Wang, X.-F. and Yakir, D.: Using stable isotopes of water in evapotranspiration studies, Hydrol. Process., 14, 14 pp., 2000.

Wassenaar, L. I., Terzer-Wassmuth, S., Douence, C., Araguas-Araguas, L., Aggarwal, P. K., and Coplen, T. B.: Seeking excellence: An evaluation of 235 international laboratories conducting water isotope analyses by isotope-ratio and laser-absorption spectrometry, Rapid Commun. Mass Sp., 32, 393–406, https://doi.org/10.1002/rcm.8052, 2018.

Welp, L. R., Keeling, R. F., Meijer, H. A. J., Bollenbacher, A. F., Piper, S. C., Yoshimura, K., Francey, R. J., Allison, C. A., and Wahlen, M.: Interannual variability in the oxygen isotopes of atmospheric CO_2 driven by El Niño, Nature, 477, 579–582, https://doi.org/10.1038/nature10421, 2011.

West, A. G., Patrickson, S. J., and Ehleringer, J. R.: Water extraction times for plant and soil materials used in stable isotope analysis, Rapid Commun. Mass Sp., 20, 1317–1321, https://doi.org/10.1002/rcm.2456, 2006.

Wiegel, A. A., Cole, A. S., Hoag, K. J., Atlas, E. L., Schauffler, S. M., and Boering, K. A.: Unexpected variations in the triple oxygen isotope composition of stratospheric carbon dioxide, P. Natl. Acad. Sci. USA, 110, 17680–17685, https://doi.org/10.1073/pnas.1213082110, 2013.

Wingate, L., Ogée, J., Cuntz, M., Genty, B., Reiter, I., Seibt, U., Yakir, D., Maseyk, K., Pendall, E. G., Barbour, M. M., Mortazavi, B., Burlett, R., Peylin, P., Miller, J., Mencuccini, M., Shim, J. H., Hunt, J., and Grace, J.: The impact of soil microorganisms on the global budget of $\delta^{18}O$ in atmospheric CO_2, P. Natl. Acad. Sci. USA, 106, 4 pp., 2009.

Yakir, D.: Oxygen-18 of leaf water: a crossroad for plant-associated isotopic signals, in: Stable isotopes: integration of biological, ecological and geochemical processes, edited by: Griffiths, H., BIOS Scientific Publishers, Oxford, 147–188, 1998.

Yakir, D. and Sternberg, L. S. L.: The use of stable isotopes to study ecosystem gas exchange, Oecologia, 123, 4 pp., 2000.

Young, E. D., Galy, A., and Nagahara, H.: Kinetic and equilibrium mass-dependent isotope fractionation laws in nature and their geochemical and cosmochemical significance, Geochim. Cosmochim. Ac., 66, 9 pp., 2002.

Yung, Y. L., DoMore, W. B., and Pinto, J. P.: Isotopic exhange between carbon dioxide and ozone via $O(^1D)$ in the stratosphere, Geophys. Res. Lett., 18, 3 pp., 1991.

Yung, Y. L., Lee, A. Y. T., Irion, F. W., DeMore, W. B., and Wen, J.: Carbon dioxide in the atmosphere: Isotopic exchange with ozone and its use as a tracer in the middle atmosphere, J. Geophys. Res., 102, 9 pp., 1997.